UNIVERSITY OF CALIFORNIA, SAN DIEGO

JACOBS SCHOOL OF ENGINEERING
LA JOLLA, CA

MAE 156B SENIOR DESIGN PROJECT REPORT

Power at Sea

Wave-Enabled Energy Generation Using Streaming Potential

BY

Mamie Grace Barnard
Ashley Campbell
Markus Gokan
Justin Kwak
Gabrielle Scott

TO

DEPARTMENT OF MECHANICAL AND AEROSPACE ENGINEERING
UNIVERSITY OF CALIFORNIA, SAN DIEGO
and
PALAEMUS OCEANIC, LLC

March 19th, 2025

Abstract

There exists a significant gap in the technological readiness of marine energy conversion technologies compared to intermittent renewables, such as solar and wind, despite their high potential as continuous energy producers. Previous research has demonstrated that an electric potential difference can be generated by flowing an aqueous electrolyte solution, such as salt water, through charged capillary channels (i.e. streaming potential). This paper expands on prior research, with the goal of developing a solid-state transducer that leverages ocean wave dynamics to generate usable electrical energy. The transducer "chip" consists of a triangular microchannel milled into the surface of a polyvinylidene fluoride (PVDF) substrate. PVDF is a ferroelectric material selected for its high dielectric constant, and the transducer chips studied successfully demonstrate that streaming potential can be observed in PVDF channels with cross-sectional areas of orders of magnitude previously unexplored. The transducer chip design was tested in single-channel, multi-channel, and single-channel multi-chip configurations using a 0.1mmol saline solution as the aqueous electrolyte. Results from testing at flow rates ranging from 4, 8, 12, and 16 GPH yielded satisfactory results of 0.19V to 1.6V, from a single channel, and exceeded the expected values from the Helmholtz–Smoluchowski equations in nearly all cases

Table of Contents

List of Figures

iv

List of Tables

Chapter 1: Introduction

1.1   Project Background

With more than 71 percent of the Earth covered by oceans, marine energy represents one of the most abundant and accessible potential sources of clean and renewable energy [1]. Ocean waves, in particular, have been identified by researchers as the "most promising form of [ocean] energy," producing potentially as much as 80,000 TW/year of energy [2]. Individually, a single wave crest can transmit an average of 10-50 kW of power per meter [2]. Despite this, ocean wave energy conversion technologies remain significantly less mature compared to other renewable energy harvesting technologies, such as solar power or wind [3]. In the global transition towards sustainable energy systems, technologies capable of converting ocean wave energy into usable electricity have increasingly become the focus of research efforts from both academia and industry.

One promising technology aims to use streaming potential, a phenomenon wherein a liquid flowing across a charged, solid surface channel creates a measurable electric field, to generate electricity. When an aqueous electrolyte solution is forced to flow through a capillary channel, ions with a charge opposite to the surface are carried away, resulting in charge accumulation and an electrical potential difference between the entrance and exit of the channel, as shown in Figure 1.1 [4].
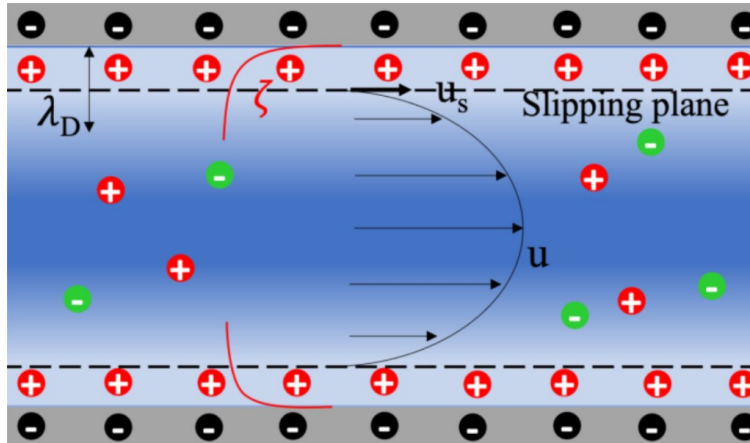
Figure 1.1: Scientific diagram of laminar flow across a charged surface

To understand this phenomenon, it is useful to consider a simple example of water moving over a flat surface. As water travels over the surface, a boundary layer forms and the dynamics of that boundary layer are well studied. However, if the fluid is not pure water, but instead a homogeneous electrolyte solution—such as salt water—and the surface is electrically charged, a second type of boundary layer forms: the Stern layer. This layer consists of the opposing ions (for example, the Na+ in salt) from the dissociated electrolyte in the water that are attracted to the charge of the solid surface. As the fluid velocity and pressure drop increase, the force of attraction between these ions and the surface becomes larger than that of the dissociated ionic bond between the Na+ and Cl-, resulting in a measurable physical separation between them in the fluid, known as interfacial polarization. This separation, multiplied over many ions across

a large surface area, can now be interpreted as a measurable electric potential difference. This scientific phenomenon forms the conceptual basis of this research and experimental design project and presents a promising avenue for the development of a novel renewable energy technology.

1.2   Existing Design Solutions

The University of California, San Diego's Bandaru Lab, in partnership with maritime sensing technology company Palaemus Oceanic, has conducted research into the streaming potential of ocean-analogous saline solutions in microchannel structures. The Bandaru Lab has been at the forefront of research that uses the electrokinetic principles driving this project. The focus of their research has been to improve upon the baseline voltages of approximately 0.04 mV/Pa produced from existing electrokinetics research [5]. This has been accomplished most recently through a study in surface roughening on the flow channel, as well as research into the outputs of multiple connecting fluid channels. The test setup used for this research consists of a microchannel assembly, a syringe pump to generate flow through the channel, attached electrodes with a multimeter for voltage monitoring, and an attached manometer for pressure readouts.
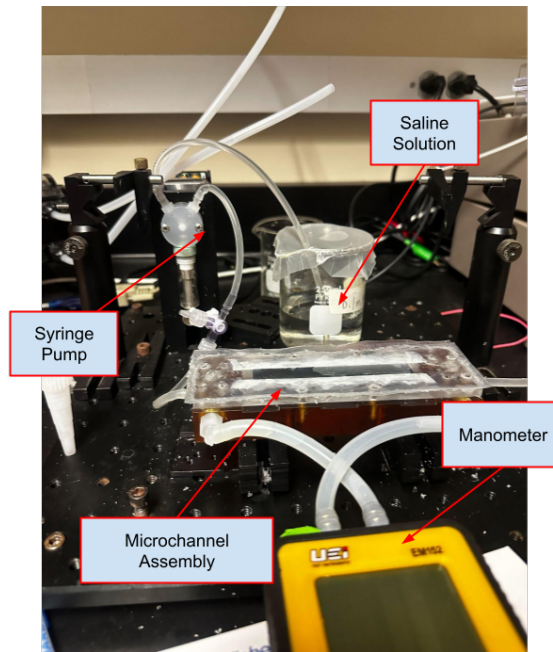
Figure 1.2: Bandaru Lab experimental set up

The microchannel assembly has three layers: an upper wall and side wall made of poly-dimethylsiloxane (PDMS) and a bottom substrate made of a silicon (Si) wafer, shown below in Figure 1.3 [5]. The channel itself is 12 cm in length and 0.9 cm in width with a height of 250 μm.
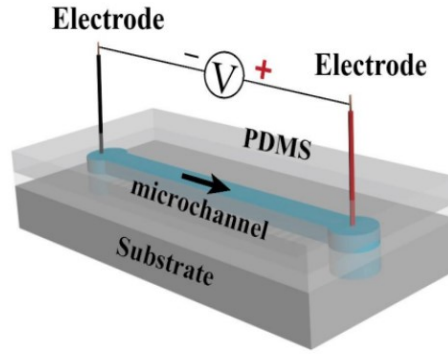
Figure 1.3: Schematic of the Bandaru Lab microchannel transducer design

For the purposes of surface roughening research, the Si wafer is etched with different patterns using photolithography. Through this research, the Bandaru Lab successfully demonstrated that an increased voltage potential can be created via interfacial polarization, generating 0.1 mV/Pa using a 0.1mM NaCl solution [6]. Additionally, they demonstrated the principle of linearly increasing voltage when microchannels were connected in series to each other [7].

The Bandaru Lab design, though functional in a controlled laboratory environment, still requires significant refinement to scale the performance and maximize the energy output of the substrate. While their research exhibits the electrokinetic principles behind this technology, as well as its improved performance as an array, there are significant areas for improvement that must be addressed in the channel design and test setup for the assembly to become a commercially viable product and allow for further research to be conducted.

The primary areas of improvement lie in the material choice, fabrication methods, and microchannel design. The material chosen for the microchannels, PDMS, is often used for microfluidics due to its transparency and ease of microfabrication methods. It is, however, a hyperelastic material that flexes under high pressure water flow, thereby restricting the testing capabilities of the channel [7]. Additionally, the microchannel design itself is difficult to mass manufacture and, if used in a practical application using a natural water source, lends itself to blockage and biofouling. This project seeks to build upon the work done by the Bandaru Lab and address the current issues in order to create a commercially viable transducer channel design, as well as a modular test fixture that allows for further research. While the basic scientific principles remain the same, improvements such as a stiffer and more suitable channel material that can handle high flow rates and pressures, a larger channel for ease of manufacturing, a transducer chip design that is conducive to mass manufacturing techniques such as injection molding, and higher voltage outputs have been the focus of the project.

1.3 Design Requirements

1.3.1 Overview of Design Requirements

The project requirements, defined based on a literature review and meetings with the Bandaru Laboratory and Palaemus Oceanic, are outlined in Table 1.1 and 1.2. Two sets of requirements were established: (1) for the design and testing of the transducer chip and (2) for the

test fixture assembly as a whole. Requirements are ranked by their relative importance to the project sponsors and will be referenced throughout the paper by a corresponding alphanumeric identifier.

1.3.2   Transducer Chip Design Requirements

Table 1.1: Transducer Chip Design Requirements

Req.	Name	Description	Testing
R.C.1	Voltage	A single transducer chip will generate more than 50mV.	Voltage testing via voltmeter.
R.C.2	Flow Velocity	The transducer chip will be capable of operating under standard ocean dynamic conditions (1-10 m/s).	Flow rate read out on test fixture.
R.C.3	Metamaterial Compatibility	Transducer chips can be interconnected, layered, meshed or composited together into a larger structure capable of surviving dynamic ocean conditions.	Demonstrate multi-cell assembly
R.C.4	System Modularity	A transducer chip stack will demonstrate consistent additive properties in series and parallel configurations.	Multi-unit testing with voltmeter.
R.C.5	Current	The transducer chip voltage potential will not reduce to zero in the presence of an applied load.	Precision resistor.
R.C.6	Mass Production	The transducer chip will be reproducible using mass manufacturing methods.	Demonstrate through injection moldable designs.
R.C.7	Biofouling	The transducer chip material will be selected to be resistant to the build-up of salt deposits and biomaterials.	In-situ testing in saltwater bath/ocean environment.

1.3.3 Test Fixture Design Requirements

Table 1.2: Test Fixture Design Requirements

Req.	Name	Description	Reasoning
R.F.1	Flow Rate Control	The test fixture shall have a precise mechanism for metering the flow of fluid during testing.	R.C.1, R.C.2, R.C.3
R.F.2	Universal Mounting	The test fixture shall be designed to test transducer chips with differing microchannel geometries.	R.C.1, R.C.2, R.C.3
R.F.3	Constant Flow	The test fixture pumping system shall be capable of maintaining a constant flow rate without stalling or otherwise failing and be able to effectively restrict flow.	R.C.1, R.C.2
R.F.4	Watertight Sealing	The test fixture shall prevent leakage across the channels during testing.	R.C.1, R.C.2
R.F.5	Fluid Reservoir	The test fixture shall be able to accommodate extended testing durations.	R.C.1, R.C.2
R.F.6	Multi-Unit Testing	The test fixture shall promote and enable the testing of multiple transducer chips in a single chip stack.	R.C.4

1.4 Deliverables

Table 1.3: Project Deliverables

Name	Description
Modular Test Bed	A watertight testing system consisting of manifolds with hose connections, a transducer chip, and clamping plates for sealing. The manifolds will be modular so a variety of transducer chips could be tested for research regarding channel geometry and material.
Test Fixture	A full test fixture including a pump, two flow meters, voltmeter, manometer, precision resistor, and ammeter. The fixture is designed with universal mounting holes to allow for additional measurement devices. Combined, the flow meters are rated for a range of 0.7 to 44 gallons per hour (GPH).
Manifold Design	CAD files, drawings, and manufacturing steps for the creation of additional manifolds to be used with future chip iterations and research.
Transducer Chips, Single Channel Design	CAD files, drawings, and manufacturing steps for the reproduction of the current PVDF chip designs for a single channel chip.
Transducer Chips, Five Channel Design	CAD files, drawings, and manufacturing steps for the reproduction of the current PVDF chip designs for a multiple channel chip.
Data	Voltage and current output data for one single channel chip for flow rates of 4, 8, 12, and 16 GPH. Voltage output data for two single channel chips stacked and wired in parallel for flow rates of 4, 8, 12, and 16 GPH. Voltage output data for one five channel chip for flow rates of 4, 8, 12, and 16 GPH.
User's Guide	A full user's guide outlining the set-up of the test bed and test fixture and data collection process. The guide includes troubleshooting techniques and advice.

Chapter 2: Final Design

2.1 Description

Previous work toward the development of streaming potential generation devices has required high-cost laboratory equipment and complex, bespoke fabrication techniques. Here, a low-cost, easily manufactured alternative is proposed, with the overarching goal of progressing the technology towards a higher technology readiness level and, eventually, towards commercial applications as an innovative renewable energy technology. The design consists of a solid-state transducer and a surrounding test fixture that simulates the interaction between the transducer chip and ocean waves in a controlled environment, facilitating experimental testing and data acquisition. During testing, a saline solution is pumped from a fluid reservoir through a constant flow pump, routes through one of two flow meters to an inlet manifold, then flows through a transducer chip micro-channel before exiting via an outlet manifold and into a wastewater beaker (Figure 2.1). A data acquisition system was used to determine the voltage, current, and pressure of the system during testing.
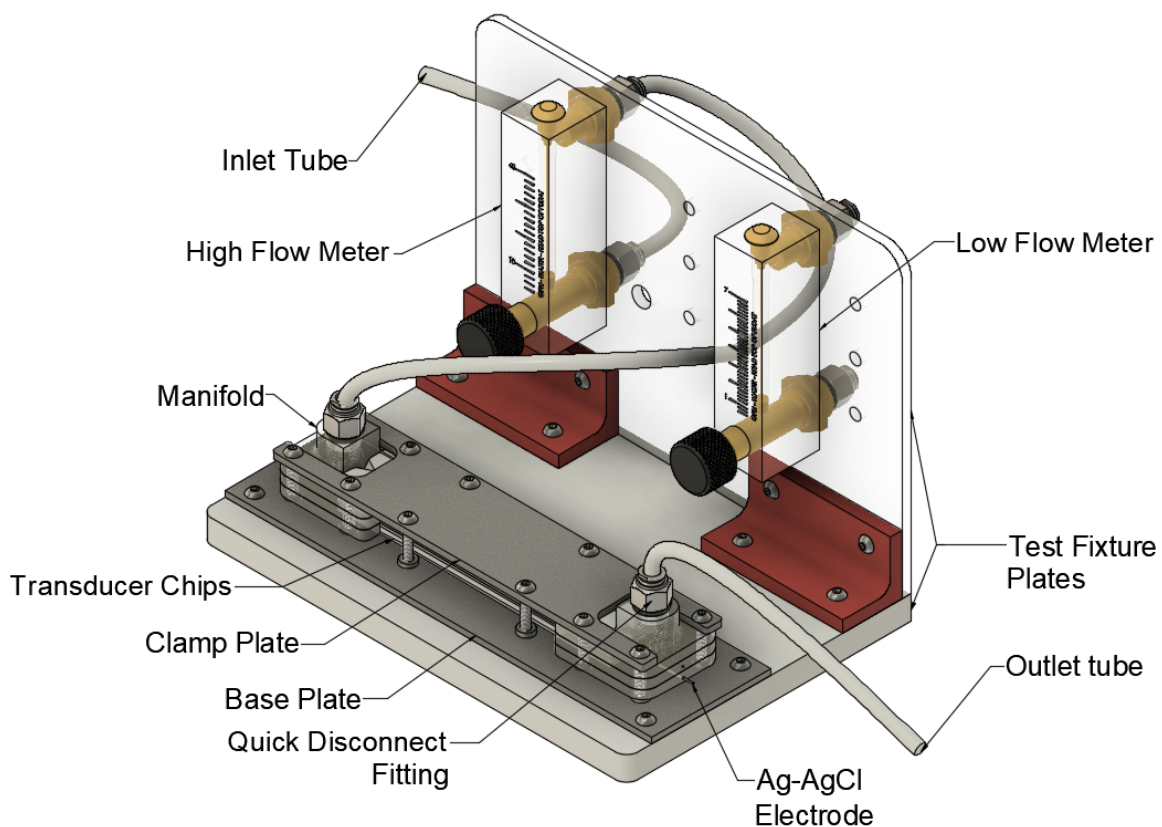
Figure 2.1: Rendered test fixture assembly with individual components labeled.

The test fixture is outfitted with two modular manifolds, a clamping and base plate, a constant flow rate pump, and two flow meters (0.7-7.7 GPH and 4.0-44.0 GPH), detailed in Figure 2.3 below.

Chapter 3: Design Components

3.1   The Transducer Chip

Central to the project's design and iteration process is the *transducer chip*, a solid-state device that converts wave energy into electricity through an electrokinetic phenomena known as streaming potential. This potential is a result of the flow of an electrolyte across a charged surface and the subsequent formation of an electrical double layer on that surface. Figure 3.1 shows how the pressure gradient of the flow, in combination with the formation of the double layer, results in a separation of the dissociated ions in the solution.
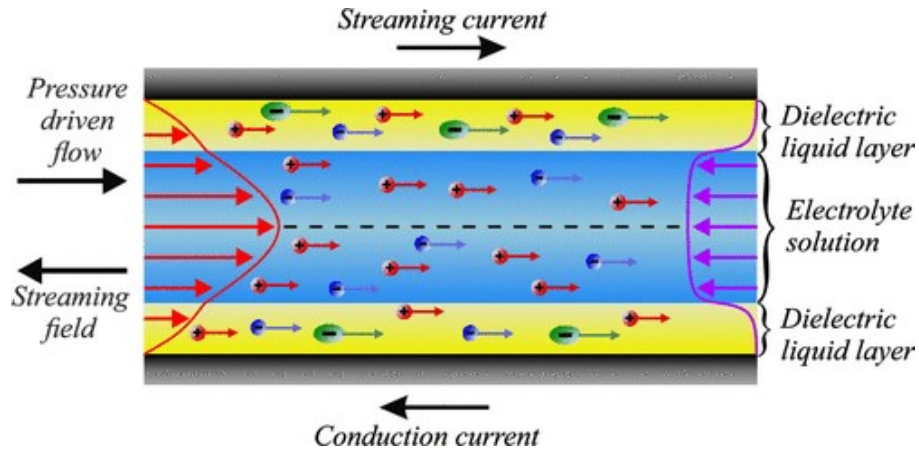
Figure 3.1: Scientific diagram of streaming potential and streaming current from pressure driven flow

There are many models with which the voltage and current generated by this double layer (commonly referred to as "streaming potential" and "streaming current" respectively) can be estimated, but the most easily understood is the Helmholtz-Smoluchowski Equations. The equations below assume a no-slip boundary condition and an electrolyte—saltwater, in this case—that is driven by a pressure gradient.

$$V_s = \frac{\varepsilon \cdot \zeta}{\mu \cdot K} \cdot \Delta P \qquad (3.1)$$

$$I_s = \frac{K \cdot \pi \cdot r^2}{L} \cdot V_s \qquad (3.2)$$

V_s : Streaming potential, V

I_s : Streaming current, A

ζ : Zeta potential, V

L : Channel length, m

r : Hydraulic radius, m

ΔP : Pressure difference, Pa

ε : Dielectric constant of the liquid

μ : Dynamic viscosity of the liquid, Pa·s

K : Specific conductivity of the bulk liquid, S/m

These variables can be divided into two classes: those fixed by environmental conditions, such as ε, μ, and K, which are properties of water, and those which can be controlled through design choices, including r, ζ, L, and ΔP. Assuming laminar flow conditions:

$$\Delta P = \frac{32 \cdot \mu \cdot L \cdot Q}{\gamma \cdot D_h^4} \qquad (3.3) \qquad\qquad K = \frac{32 \cdot A^2}{\gamma \cdot D_h^4} \qquad (3.4)$$

μ : Dynamic viscosity of the fluid, Pa·s

L : Length of the channel, m

Q : Volumetric flow rate, m^3/s

D_h : Hydraulic diameter, m

γ : Poiseuille shape factor

This, combined with the Helmholtz-Smoluchowski Equations, yields:

$$V_s = \frac{\varepsilon \cdot \zeta \cdot L \cdot Q}{A^2} \qquad (3.5) \qquad\qquad I_s = \frac{8 \cdot \pi \cdot \varepsilon \cdot \zeta \cdot Q}{\gamma \cdot D_h^2} \qquad (3.6)$$

Here, it becomes helpful to further distinguish the design variables into two additional categories: material properties: ζ, and channel properties: A, γ, L, D_h.

Property	Effect on V_s	Effect on I_s	General Relationship to Other Properties
Zeta Potential, ζ	Increases	Increases	N/A
Cross Sectional Area, A	Decreases (squared)	N/A	Proportional to Hydraulic Diameter
Poiseuille Shape Factor, γ	N/A	Decreases	Inversely Proportional to Hydraulic Diameter
Channel Length, L	Increases	N/A	N/A
Hydraulic Diameter, D_h	N/A	Decreases (squared)	Proportional to Cross Sectional Area

Table 3.1: Summary of Relationships Between Key Properties and Streaming Potential and Streaming Current

Referring to Table 3.1, the following trends become clear: maximize ζ and L, while minimizing A, γ, and D_h to achieve maximum streaming current and potential. Zeta potential is defined as the electrical potential at the plane of shear, better defined as between the first layer, or surface charge, of the EDL and the inherent charge that the material possesses. The quantity of charge that can accumulate on the surface is directly related to the relative permittivity of

the material. More specifically, it is the difference between the dielectric constant of the material and the electrolyte. Succinctly: the dielectric constant of the material should be increased up to the point of matching the electrolyte to maximize charge accumulation at the surface. Conversely, the Poiseuille shape factor can be considered less important than the hydraulic diameter and cross-sectional area due to the latter two being of higher degree and proportional to each other. Combining these conclusions results in clear and orderly design requirements for the transducer's channel:

- High Dielectric Constant

- Long Channel Length

- Low Cross Sectional Area and Hydraulic Diameter

- Low Poiseuille Shape Factor

Shape	Hydraulic Diameter D_h	Cross-Sectional Area A	Poiseuille Shape Factor γ	Overall Consideration
Thin Slit (Parallel Plates)	$2S$	$S \cdot W$	Very high $(\gg 28.4)$	Too high γ, impractical for balancing all three.
Equilateral Triangle	$\frac{\sqrt{3}}{3}S$	$\frac{\sqrt{3}}{4}S^2$	21.2	low D_h, moderate γ.
90°-45°-45° Triangle	$(\sqrt{2}-1)S$	$\frac{1}{2}\left(\frac{S}{\sqrt{2}}\right)^2$	26.3	More resistance than equilateral triangle, larger γ.
Square Channel	S	S^2	28.4	Larger D_h, so less ideal.
Circular Pipe	S	$\frac{\pi}{4}S^2$	16	Lowest γ, but highest D_h for a given size.

Table 3.2: Comparison of Different Shapes Minimizing D_h and A with Reduced Weight on γ

Selection of an ideal transducer chip material and the optimal microchannel geometry was essential for maximizing voltage generation during testing. The thermoplastic fluoropolymer, polyvinylidene fluoride (PVDF), was chosen as the material for the transducer chip due to its high dielectric constant, low cost, good mechanical properties, and compatibility with a variety of manufacturing methods, such as machining and injection molding; all of which are key considerations when advancing to a further technology readiness level. Additionally, PVDF

is capable of being composited with a variety of other materials to further refine the dielectric properties of the transducer, though this option was not explored in this work. The use of PVDF represents a significant deviation from most previous implementations of streaming potential for electricity generation, which have traditionally been constructed with silicone wafers (parallel plate configurations), sintered glass (porous medium), or polydimethylsiloxane– PDMS (microfluidic channels). These materials may have higher dielectric constants, but do not meet the survivability requirements of **R.C.2**.

Single Channel Layout　　**Five Channel Layout**　　**Bottom View**
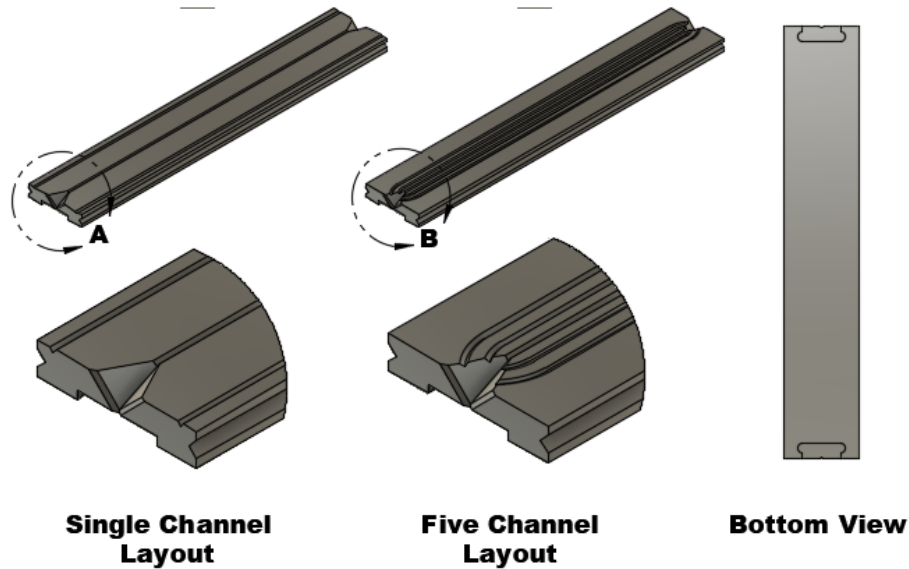
Figure 3.2: Final design of single and multi-channel PVDF transducer chips

The decision to go with a 90-45-45 triangle channel geometry was based on this as well, despite the table indicating that the equilateral triangle meets the requirements more directly. This geometry corresponds to a higher flow resistance and subsequent higher shear force at the wall, which has been shown by existing literature to improve the effect of electrical double layers. This geometry also lends itself to routine 3-axis CNC machining, as the feature can be engraved easily using a 45-degree chamfer end mill. Previous work has centered on micro- and nano-scale channels, but these configurations raise significant concerns when the goal of ocean-implementation is introduced, due to the rapid biofouling and clogging which will occur in channels of this scale in a non-laboratory environment. As such, this work was guided by the goal of identifying millimeter scale channel geometries that still yield measurable voltage.
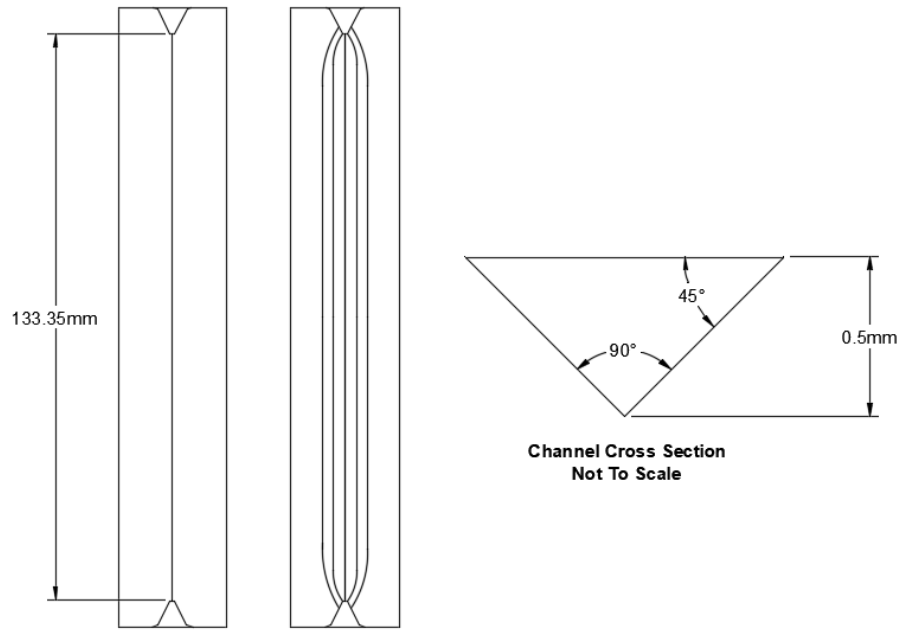
Figure 3.3: Top view of single and multi-channel PVDF transducer chip channel paths and triangular cross-sectional microchannel geometry

3.2 The Manifold

A manifold structure was designed to channel the saline solution from the pump system through the transducer chip microchannel and to route electrodes for measuring the electric potential difference across the transducer, as shown in Figure 3.4.
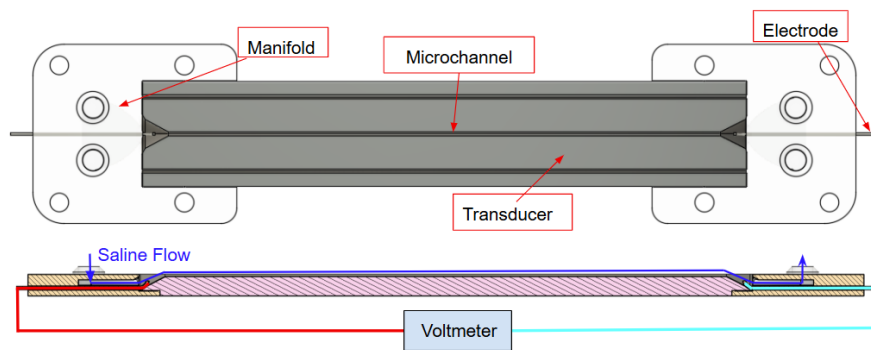
Figure 3.4: Top side views of manifold units with transducer chip showing flow across the channel.

The manifold is comprised of three distinct components: a top unit, a bottom, or base, unit, and a universal middle unit, shown in Figure 3.7. For the purposes of testing a single transducer chip sufficient to fulfill the **R.C.1** requirement, it is only necessary to assemble the manifold structure with the top and base units. To test for additive voltage properties across

multiple interconnected chips, as set forth by **R.C.3** and **R.C.4** requirements, one or more of the universal middle manifold units can be inserted between the top and base units.

All manifold units were designed with identical interfaces for mating with the transducer chips, which are seated and tightly sealed between a respective inlet and outlet manifold, per **R.C.2**.
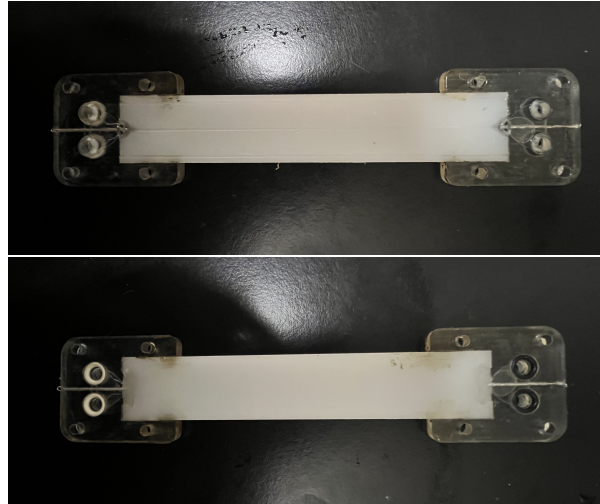
Figure 3.5: Top and bottom faces of two middle unit manifolds with transducer chip installed. O-rings visible on bottom side.

The manifold components each feature a rectangular boss extrusion designed to couple with a corresponding female recess machined into the bottom of the transducer chip. Key slot features on the manifolds were designed at the interface between the two components. V-grooves interlocking with the keyed features were machined into the sides of the transducer chip, securing and precisely aligning the three components when assembled, as shown in Figure 3.5. To prevent fluid leakage, UV-cured epoxy resin was applied along the mating surfaces of the chip and manifolds. Additionally, a 10A durometer, 0.010" thick silicone rubber strip was centered over two V-grooves machined into the transducer chip face to act as a gasket seal between the top and bottom faces of the stacked chips, as seen in Figure 3.6.
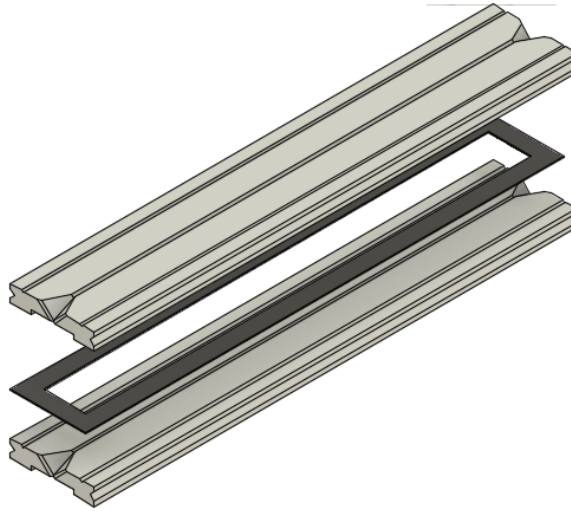
Figure 3.6: Silicone rubber gasket seal between two transducer chips. V-groove channels on the top and side faces of the transducer chip are visible.

The manifold's top unit is designed to connect to brass quick-disconnect fittings via teflon-sealed ¼" NPT threads, allowing the saline solution to flow from the fluid reservoir down into the manifold component stack. Viton® fluoro-elastomer O-rings seated in between manifold layers prevent fluid seepage at the interfaces of the manifold fluid pathways. An internal fluid channel in the middle and base manifold units diverts the flow ninety degrees, forcing the saline solution to flow out into the transducer chip microchannel. The middle unit features an 'open' T-junction diverter design, directing fluid both down and through the transducer chip, while the base unit features a 'closed' L-junction diverter, as seen in Figure 3.7. This design allows for modular stacking capabilities with multiple chips in the same assembly, enabling testing of the **R.C.4** requirement and fulfilling the **R.F.6** requirement.
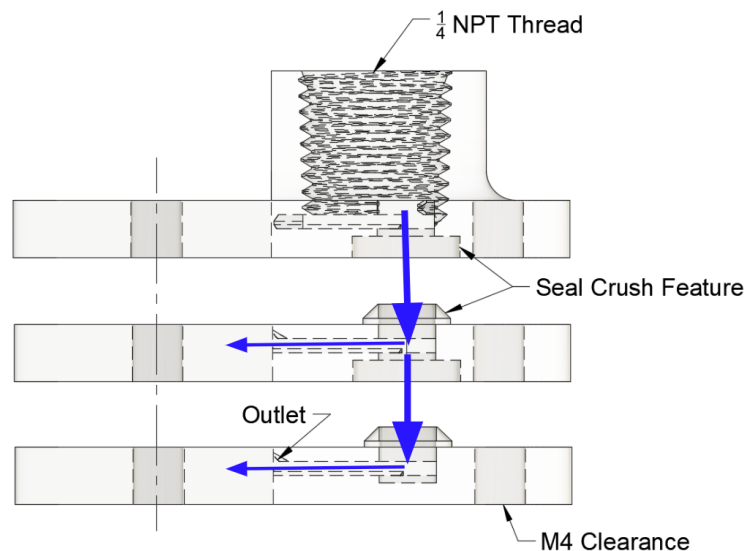
Figure 3.7: Diagram of fluid flow through manifold components

When the saline solution passes through the manifolds and is injected into the channel, two Ag-AgCl reference electrodes fixed to the manifolds become submerged in the fluid at the beginning and end. These electrodes were used to measure the resultant electric potential difference across the length of the transducer chip from the fluid flow, per R.C.1 and R.C.4 and as shown in Figure 3.8.
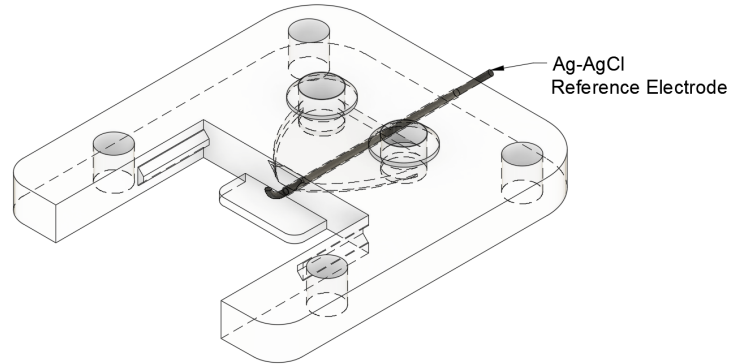
Figure 3.8: Reference electrode encased by surrounding manifold unit

3.3 Clamping Plates

The manifold and transducer chip assembly is secured between two laser cut 1/8" thick steel plates using M4 hardware, shown in Figure (image of plate assembly with top, base labeled). The clamping force of the screws on the plates prevents leakage in between the layers of transducer chips. The steel base plate, additionally, mounts directly to the larger test fixture assembly via the mounting holes in each corner (**R.F.2**). Self-clinching nuts, seen in Figure 3.9, were installed in the base plate to enable single-tool assembly and disassembly of the clamping fixture during testing.
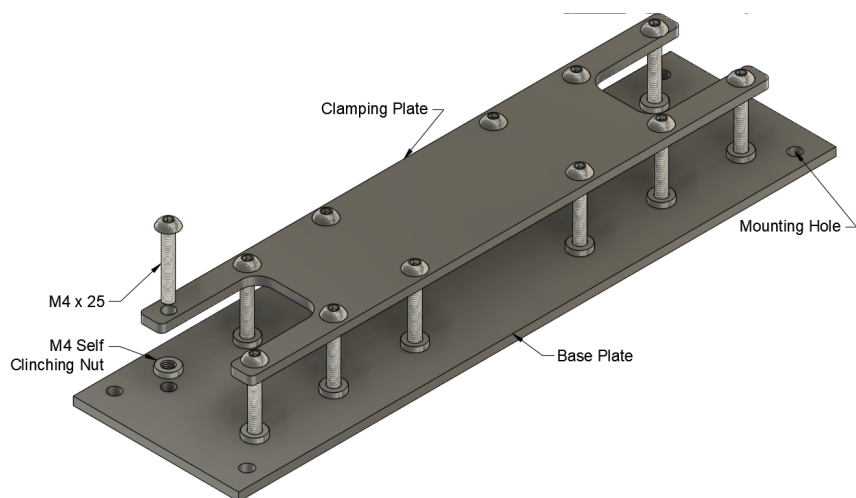
Figure 3.9: Base and clamping plate CAD model for manifold-transducer chip assembly
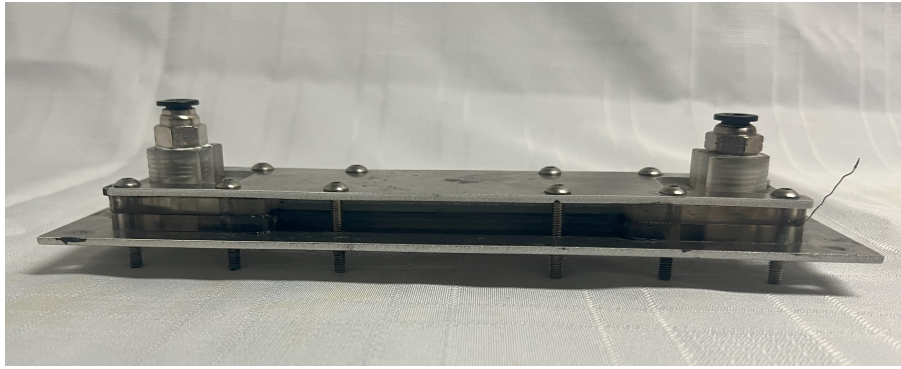
Figure 3.10: Assembled single manifold-transducer chip with clamping plates
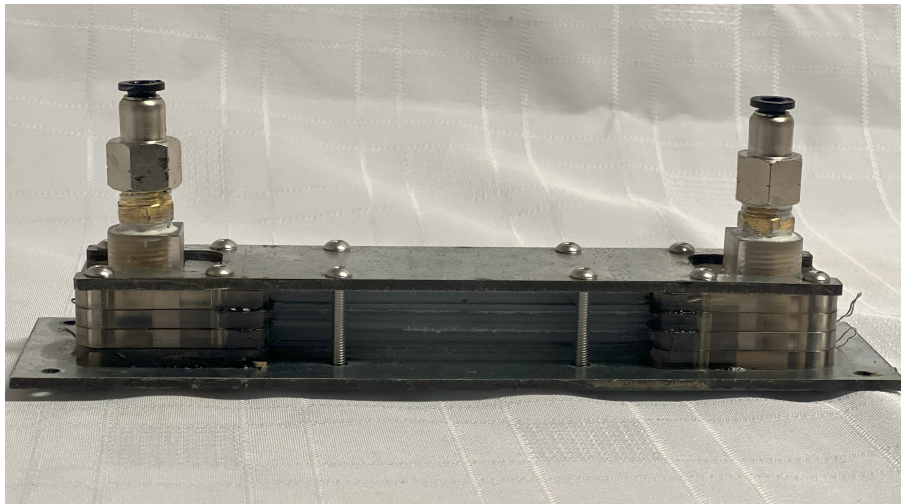
Figure 3.11: Assembled manifold-transducer multi-chip stack with clamping plates

3.4   Test Fixture

In order to test different chip designs and varying flow velocities, it was necessary to develop a test fixture that could provide constant, precisely metered flow of saline solution to the transducer chips for testing and to collect the resulting data from those experiments. These requirements necessitated three key components, (1) a constant flow pump, (2) a flow metering system, and (3) a data acquisition system, each of which plays an essential role in fulfilling the functional requirements outlined in the Test Fixture Design Requirements table.
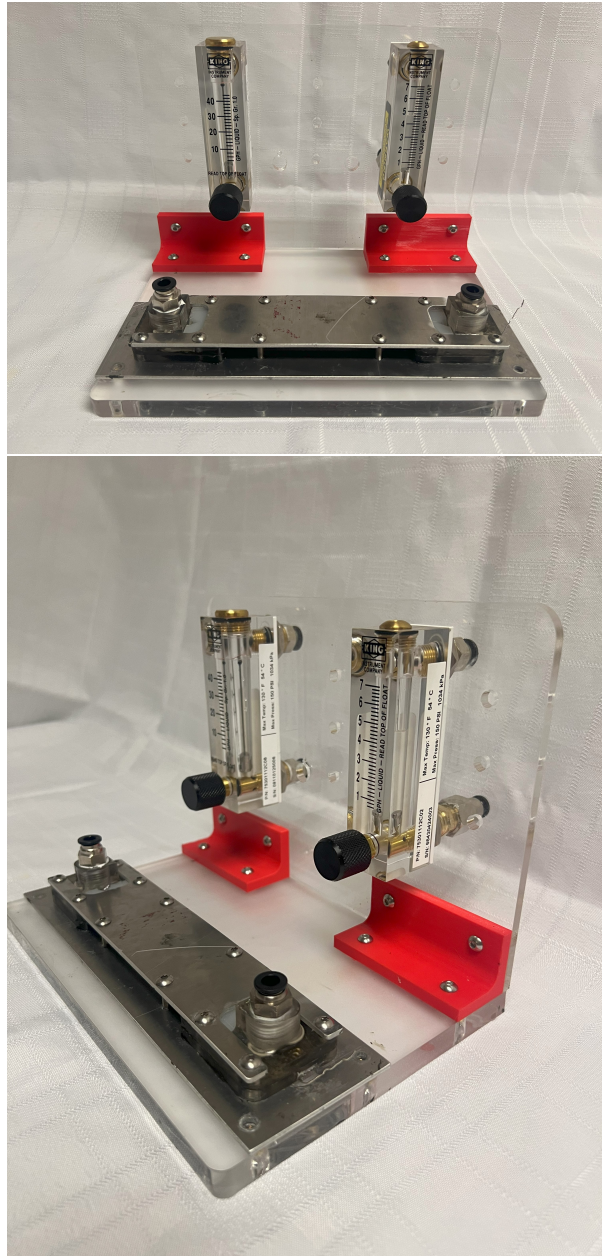
Figure 3.12: Experimental test stand with manifold-transducer chip assembly.

First, a range of channel configurations that would provide a comprehensive dataset was identified: 1, 2, 3, 5, 10, and 15 channels; as well as a minimum range of representative flow rates corresponding to free stream velocities within the channel of 1 to 10 meters per second. To achieve the same free stream velocity in multiple parallel channels, it is necessary to scale the volume flow rate proportionally to the increase in channel count. The goal, then, was to develop a flow metering and control system capable of simulating these flow conditions consistently as the channel count is increased.

The precision of a flow meter is inversely proportional to the range for which it is designed to operate in, and as such, a flow meter capable of measuring the maximum flow rates specified are not appropriate for the finer control necessary for single channel and low flow velocity

conditions. To compensate for this, the full range of flow conditions are covered by two flow meters rather than one, 0.7-7 GPH and 4-44 GPH respectively, and coverage of all but two desired flow rates was achieved, effectively fulfilling the **R.F.1** goal. Flow rates within the bounds of the respective flow meters are represented in Figure 3.13 as green cells, and red cells exceed either the upper or lower bound of the flow meter.

Flow Meter Range: 0.7-7GPH										
Channels:	1 m/s	2 m/s	3 m/s	4 m/s	5 m/s	6 m/s	7 m/s	8 m/s	9 m/s	10 m/s	Graduation
1	0.24	0.48	0.71	0.95	1.19	1.43	1.66	1.90	2.14	2.38	0.24
3	0.71	1.43	2.14	2.85	3.57	4.28	4.99	5.71	6.42	7.13	0.71
5	1.19	2.38	3.57	4.76	5.94	7.13	8.32	9.51	10.70	11.89	1.19
10	2.38	4.76	7.13	9.51	11.89	14.27	16.64	19.02	21.40	23.78	2.38
15	3.57	7.13	10.70	14.27	17.83	21.40	24.96	28.53	32.10	35.66	3.57
Flow Meter Range: 4-44GPH										
Channels:	1 m/s	2 m/s	3 m/s	4 m/s	5 m/s	6 m/s	7 m/s	8 m/s	9 m/s	10 m/s	Graduation
1	0.24	0.48	0.71	0.95	1.19	1.43	1.66	1.90	2.14	2.38	0.24
3	0.71	1.43	2.14	2.85	3.57	4.28	4.99	5.71	6.42	7.13	0.71
5	1.19	2.38	3.57	4.76	5.94	7.13	8.32	9.51	10.70	11.89	1.19
10	2.38	4.76	7.13	9.51	11.89	14.27	16.64	19.02	21.40	23.78	2.38
15	3.57	7.13	10.70	14.27	17.83	21.40	24.96	28.53	32.10	35.66	3.57

Figure 3.13: Flow rate calculations.

Using the upper bound of this range, 35.66 GPH, as a guide, it was necessary to source a continuous flow pump capable of supplying at least this amount of fluid. The pump chosen for use in the test bed setup is traditionally used for drinking water systems and was chosen for its low cost, maximum flow rate of 38 GPH, operating pressure of 60 PSI, and built-in anti-backflow valve, which allows the pump to be metered with the flow meter setup discussed above without stalling or damage (**R.F.3**). Additionally, it operates with a standard 1/4 inch outer diameter flexible plastic tubing, compatible with readily available quick disconnect fittings. Originally, a Stenner Model 45m5 peristaltic pump was employed for preliminary testing, however, the pulsatile nature of peristaltic pumps resulted in a significant oscillation in the voltage generated when the pump was on. Figure ? shows data collected using this pump: although there was still a distinct difference between the 'pump on' and 'pump off' states, a steadier and more sustained peak was deemed critical for conducting further testing.
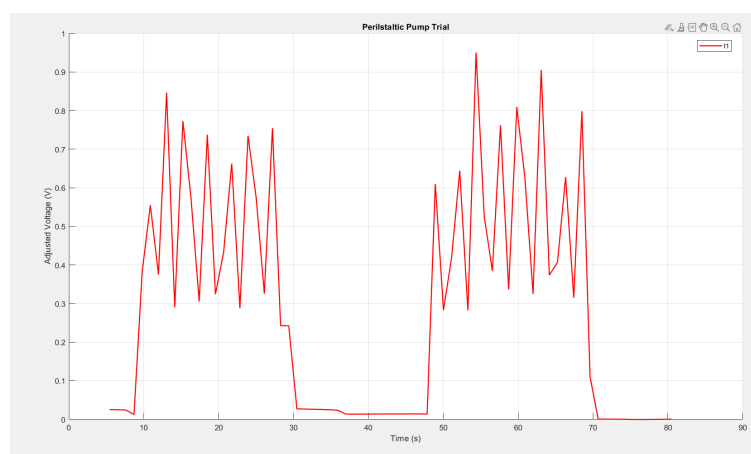
Figure 3.14: Representative peristaltic pump data from initial experiments.

A five-gallon commercial hard plastic water jug was selected as a fluid reservoir sufficiently large enough for continuous testing, per **R.F.5**.
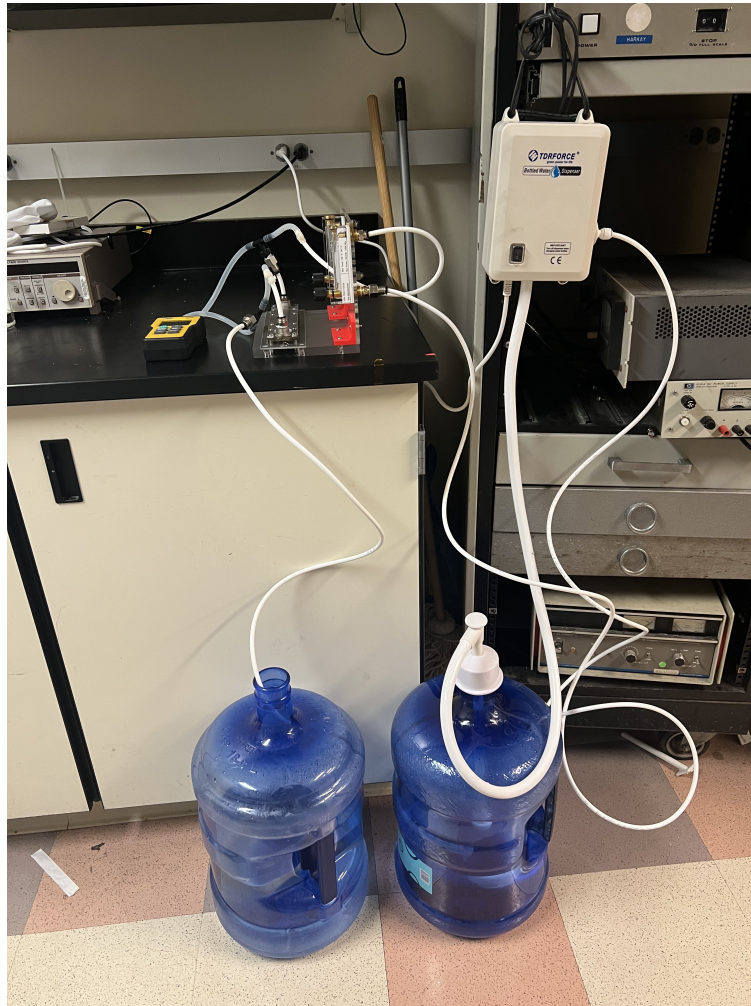
Figure 3.15: Test fixture with fluid reservoir, fluid wastewater sink, and constant flow rate pump.

The final component of the test fixture is the data acquisition equipment, which provides the necessary data required to solve and validate the streaming potential and current equations discussed at the beginning of Chapter 3. A UEi Test Instruments EM152 dual differential manometer measures the pressure drop across the test fixture up to 20 PSI, sufficient to test a single channel at low flow rates in order to establish a trend to be extrapolated further. The streaming potential is measured using a Keithley 2700 Multimeter/Data Acquisition system, capable of measuring potentials as low as 100nV at a resolution of 0.1 microvolts. It is also compatible with serial communication to a laptop running the LabView software, enabling recording and plotting of data points.
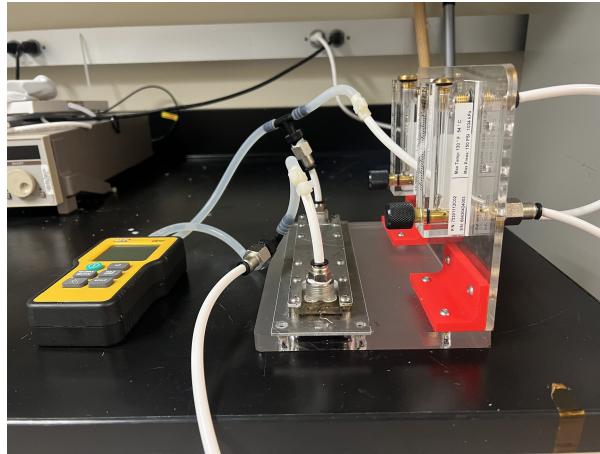
Figure 3.16: Test fixture with manometer and related tubing.

The streaming potential is measured using a Keithley 2700 Multimeter/Data Acquisition system, which is capable of measuring potentials as low as 100nV at a resolution of 0.1 microvolts. It is also compatible with serial communication to a laptop running the Labview software, enabling recording and plotting of data points.
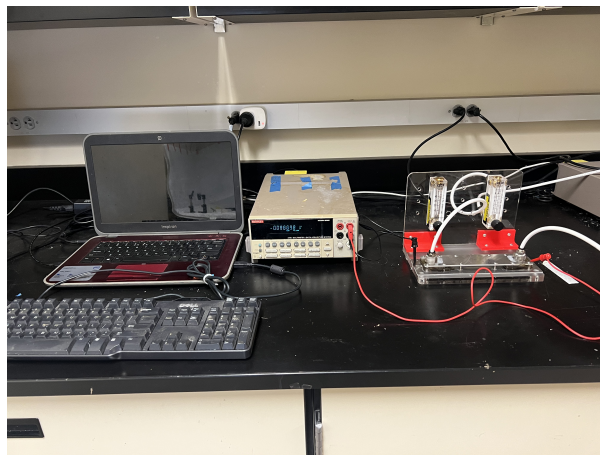
Figure 3.17: Test fixture with data acquisition equipment.

Chapter 4: Performance Analysis

4.1 Methodology

4.1.1 Test Schematic
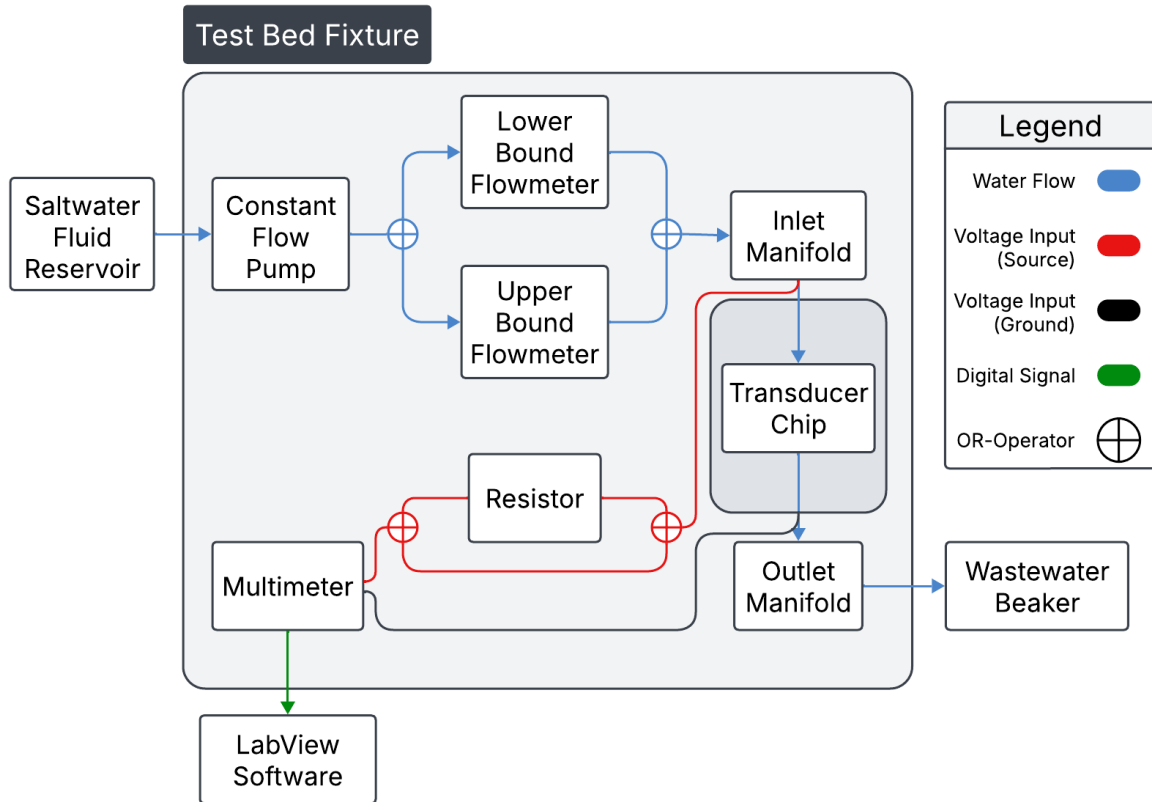
Figure 4.1: Schematic of experimental set-up for transducer chip design testing.

4.1.2 Test Set Up

1. The transducer chips, manifolds, clamping plates, quick disconnect fittings, and sealing components are assembled and firmly tightened.

2. The transducer chip and manifold assembly is fastened to the experimental test stand using M4 hardware.

3. A 0.1 mmol concentration saline solution is prepared using deionized water.

4. The appropriate flow meter is selected based on the quantity and type of transducer chip being tested, and connected to the constant flow rate pump and the inlet manifold fitting via flexible tubing.

5. Tubing is connected to the outlet manifold and routed to the wastewater reservoir, as well as between the fluid reservoir and the pump.

6. The reference electrodes mounted in the manifolds are connected to the Keithley 2700 Multimeter using hook-style test probes.

7. The multimeter is turned "ON" and given time to stabilize.

A diagram of the complete test setup can be found in Figure 4.1.

4.1.3   Test Procedure

1. Flow meter knob was adjusted to the desired gallons per hour.

2. With the pump off, the Labview software was set to read a multimeter input at a sample frequency of 1 second.

3. After the indicator beep from the multimeter signaling that sampling began, the pump was kept off for 30 seconds.

4. Constant flow pump was switched to "ON." The flow meter was monitored and adjusted to ensure minimal variation from the chosen flow rate.

5. Water was allowed to flow through the test fixture for a period of 30 seconds.

6. Pump was then switched "OFF" for a period of 30 seconds.

7. This process was repeated for a total of 210 samples, at which point the Labview application terminated data collection.

8. The resulting data reflects four 'pump off' periods and three 'pump on' periods.

Figure 4.2: Physical assembly of experimental set-up with constant flow pump, fluid reservoir, and wastewater beaker.

This testing process was repeated for a single-channel transducer chip at 4, 8, 12, and 16 GPH, as well as for two single-channel transducer chips in a stacked configuration at the same flow rates. Data underwent minor processing prior to figure creation using the MATLAB scripts included in the appendix. The first and last 5 data points were trimmed to compensate for occasional false readings when LabView connected to the multimeter. Additionally, the steady-state voltage of the system is not 0V and can be inconsistent between trials. To compensate for this, the first 20 values of each modified data set were averaged (corresponding to the first region where the pump is off), and that average was subtracted from all data values to shift the data down the X-axis. Figure 4.3 shows a representation of the data graphed before and after the adjustment process.
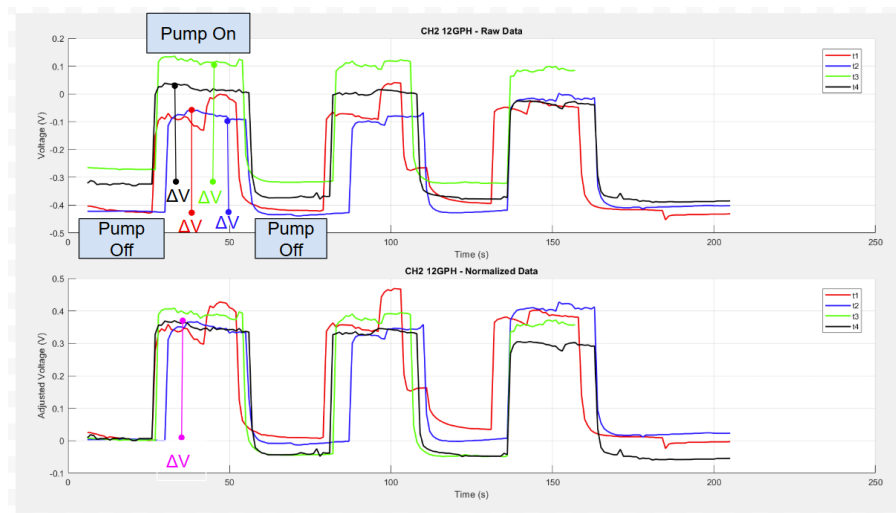
Figure 4.3: Graph of data pre-offset and with normalization around zero.

The figures presented are produced with data taken in this method, and share the same low-high voltage pattern where low points correspond to regions of the pump being off. The V used in calculation are found by averaging the values of the pump-on periods for all four trials using the adjusted data sets.

4.2 Results
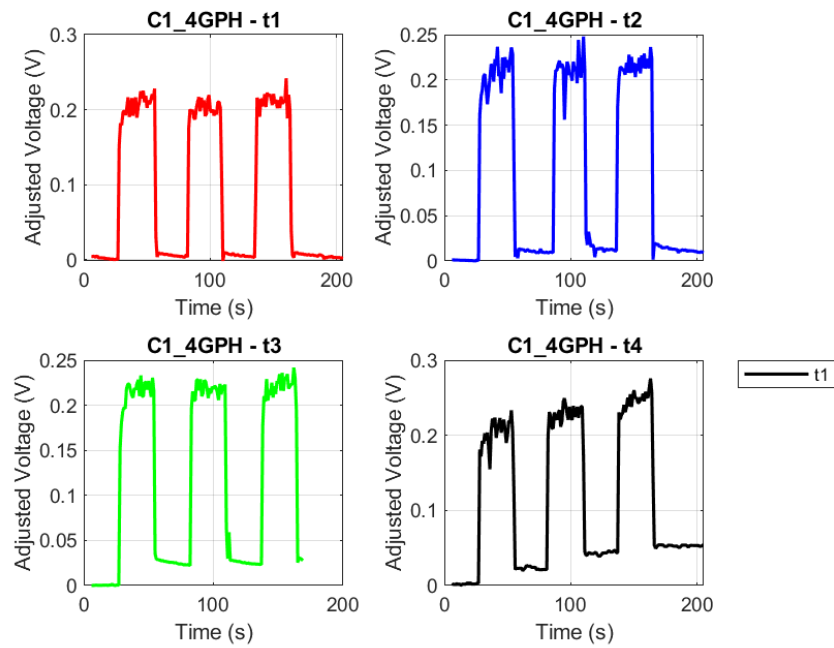
Figure 4.4: Voltage measurements for single channel flow at 4 GPH
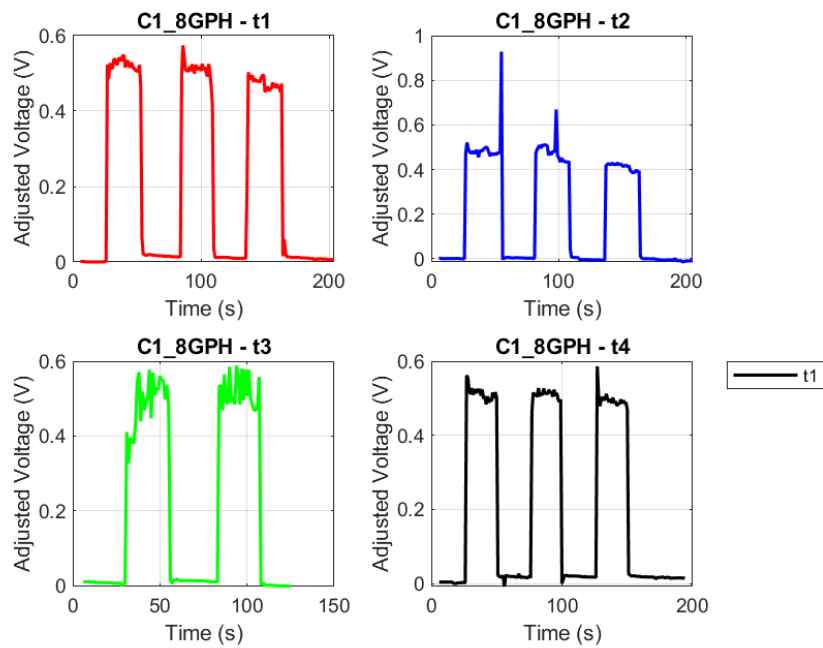
Figure 4.5: Voltage measurements for single channel flow at 8 GPH
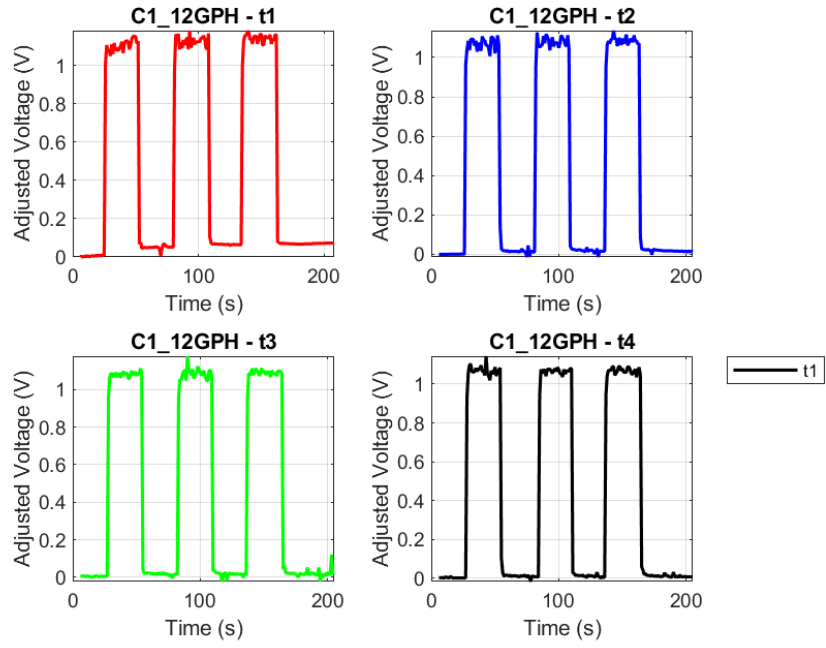
Figure 4.6: Voltage measurements for single channel flow at 12 GPH

Figure 4.7: Voltage measurements for single channel flow at 16 GPH

Figure 4.8: Voltage measurements for double channel flow at 4 GPH

Figure 4.9: Voltage measurements for double channel flow at 8 GPH

Figure 4.10: Voltage measurements for double channel flow at 12 GPH

Figure 4.11: Voltage measurements for double channel flow at 16 GPH

4.3   Analysis

The above data shows the voltage potential sampled by the voltmeter in 1-second intervals graphed against time for 210 seconds over a period of four trials. In each trial, the pump was
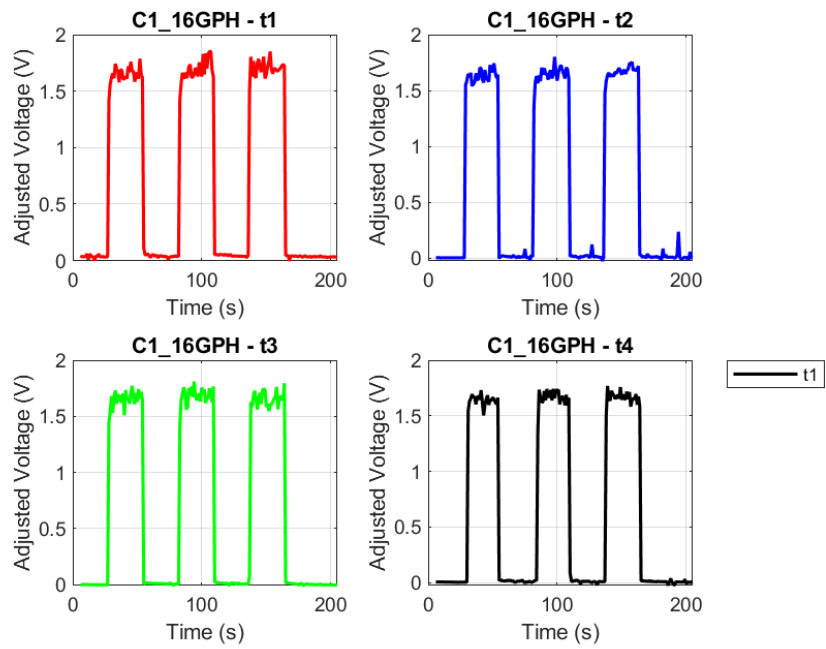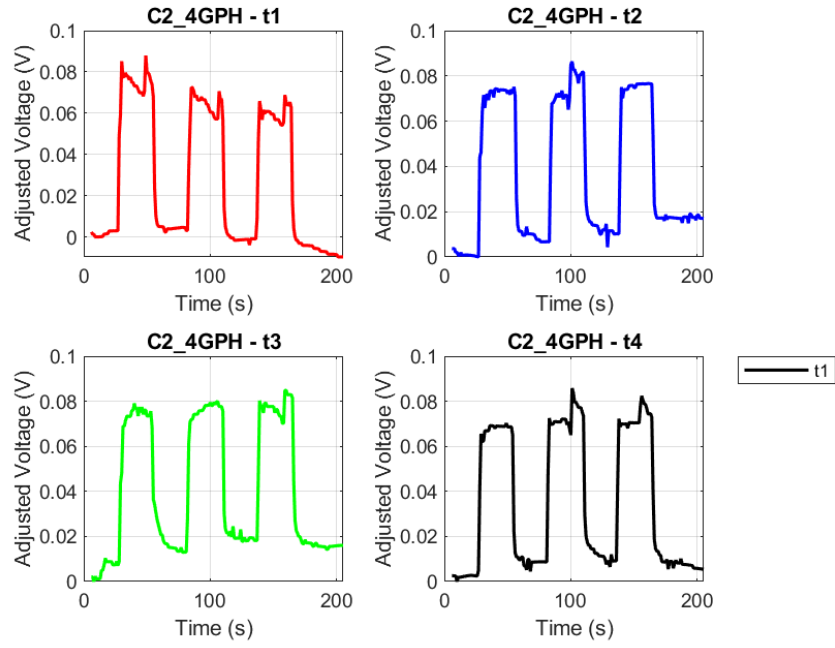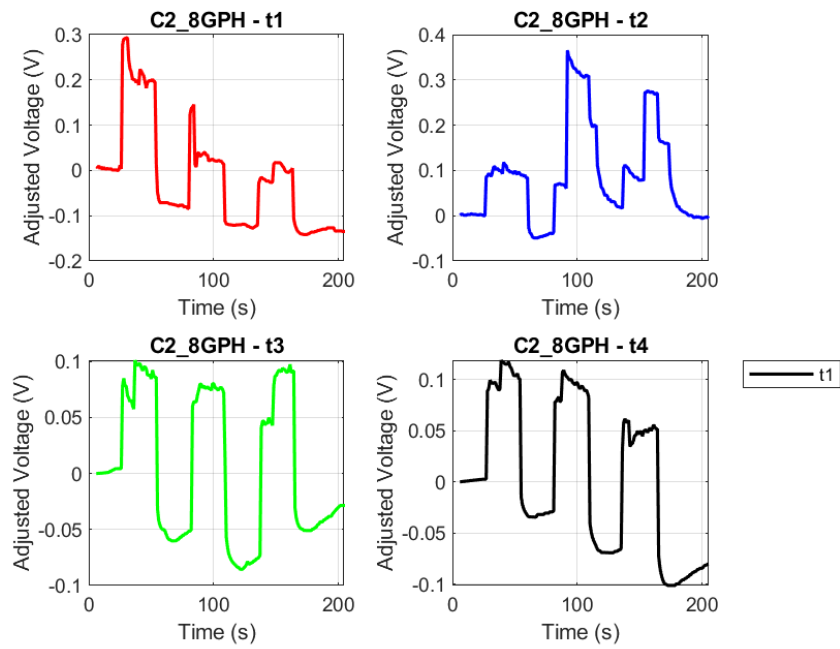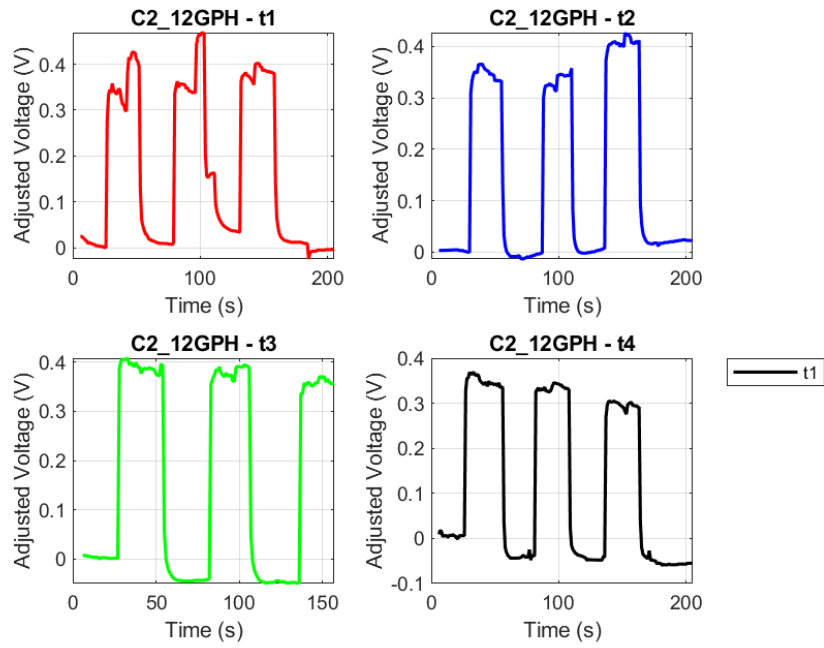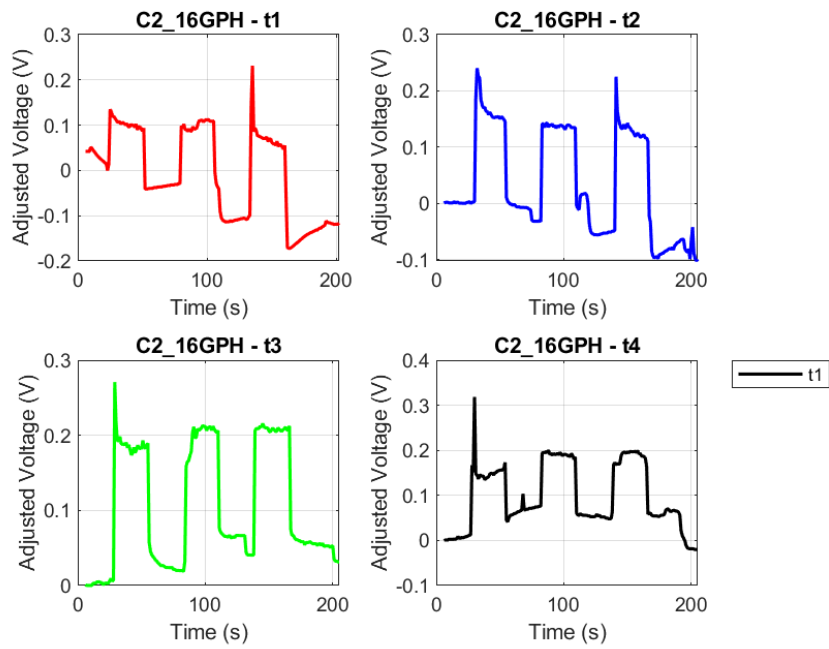
initially turned off and then turned on and off in 30-second intervals for the duration of the testing period.

In the single channel configuration, a very clear upward trend is visible as flow rate increases, what is interesting to note, however, is that the transducer displays, roughly, a voltage scaling factor of 3:2 with respect to the flow rate, which is distinctly better than the 1:1 relationship that the Helmholtz-Smoluchowski Equations indicate. Further trials must be conducted due to significant measurement error in the two channel configuration and to more clearly map the behavior of the system in multi-channel configurations.

Pressure drop at 4 GPH across the single channel configuration ranged from 12.75-13.3KPa and in the double channel configuration a similar range of 11-11.3 KPa was observed through all 4 trials. This is consistent with Darcy-Weisbach principals, as the volume flow rate was maintained while doubling the flow area resulting in a lower fluid velocity.

These results can be validated by recalling the Helmholtz-Smoluchowski Equations now that the unknown values have been resolved taking the 1 channel, 4 GPH trials as the reference:

$$V_s = \frac{\varepsilon \cdot \zeta \cdot L \cdot Q}{A^2} \tag{4.1}$$

This equation can be rearranged to become:

$$\zeta = \frac{V_s \cdot A^2}{\varepsilon \cdot L \cdot Q} \tag{4.2}$$

- V_s – Streaming potential = 0.1876 V

- ζ – Zeta potential, V

- L – Channel length = 0.13335 m

- ε – Dielectric constant of the liquid $\approx$ 80

- Q – Volumetric flow rate = 4.206×10^{-6} m^3/s

- A – Cross-sectional area = 2.5×10^{-7} m^2

- γ – Poiseuille shape factor = 26.3

- D_h – Hydraulic diameter = 0.000414 m

Rearranging to solve for yields:

$$\zeta = \frac{V_s \cdot A^2}{\varepsilon \cdot L \cdot Q} = 2.61 10^{-10} \tag{4.3}$$

Back substituting this to predict the voltage generated by a two-channel configuration, assuming that parallel configurations are treated as increased area, results in:

$$V_s = \frac{\varepsilon \cdot \zeta \cdot L \cdot Q}{A^2} = 0.0234V \tag{4.4}$$

Table 4.1: Comparison of Theoretical and Experimental V_s Results for Single Channel (SC) and Double Channel (DC) Configurations

Q (GPH)	SC Theoretical	SC Experimental	DC Theoretical	DC Experimental
4	0.187375 V	0.1876 V	0.046844 V	0.0588 V
8	0.374751 V	0.4837 V	0.093688 V	0.1236 V
12	0.562126 V	1.0620 V	0.140532 V	0.3047 V
16	0.749502 V	1.644 V	0.187375 V	0.1415 V

In the single channel configuration, a very clear upward trend is visible as flow rate increases, what is interesting to note however is that the transducer displays, roughly, a voltage scaling factor of 3:2 with respect to the flow rate, which is distinctly better than the 1:1 relationship that the Helmholtz-Smoluchowski Equations indicate. In the two channel configuration, a significant drop in performance is observed, which is to be expected considering the area-doubling effect that parallel configurations of channels have. The voltage generated is, in effect, equivalent to what is expected from a channel depth of 0.707 mm.

Similarly solving for streaming current from the Helmholtz-Smoluchowski Equations yields:

$$I_s = \frac{8\pi\varepsilon\zeta Q}{\gamma D_h^2} = \frac{8\pi \times 80 \times 2.61 \times 10^{-10} \times 4.206 \times 10^{-6}}{26.3 \times 0.000414^2} = 4.90 \times 10^{-7} A \qquad (4.5)$$

The external current measured in the experimental setup was on the order of 10-12 Amperes AC, which is many orders of magnitude off of the expected value above. When measurements were taken attempting to measure DC current, no discernible value was measured, though, there is a high chance this is due to the experimental setup and calculation approach than it is the phenomena itself.

Chapter 5: Conclusions

5.1   Further Recommendations

This technology has been developed with the goal of achieving steady state energy generation using wave energy. This could be in the context of augmenting and supplying the power grid of cities or entire nations, or it could provide a reliable source of energy for deep sea and offshore sensing instrumentation. Currently, these technologies are limited by the size and weight of batteries, and the need to recharge or replace them as they exceed their service life. Solid-state technology such as these transducers could pave the way for a permanent energy solution as fossil fuels are phased out.

Depending on the need being met, when deployed, these transducers would likely need to be linked in massive arrays, containing thousands or tens of thousands of meters of microchannel on a multitude of transducer chips. This might be achieved by assembling a 'net' of transducers bound together with flexible joints, floating at or near the surface of the ocean or anchored perpendicularly to deep sea currents to supply flow. Or, the microchannels could be oriented vertically, with a buoy and anchor situated at opposite ends, moving the transducer up and down with the motion of the waves. In low voltage sensing applications for instrumentation, it might be possible to meet power needs with only a few individual transducers, or even a bespoke microchannel designed to meet the specific needs and form factor of the instrumentation in question.

The goal of this project was to develop a functioning transducer using a larger channel than has been attempted in previous research and a testbed capable of supporting it. What comes next is testing the limits of this technology through a range of conditions and orientations to better understand its capabilities and potential applications. First and foremost is the matter of measuring current generation by the device and developing a power density metric for use in comparison to other renewable energy sources. Additionally, alternative and advanced manufacturing methods can be used to facilitate mass production such as injection molding or to boost performance through increasing the dielectric constant of the material such as compositing PVDF with another material or surface plasma treatment which has proven to augment the formation of electrical double layers and increase streaming potential.

5.2   Safety Considerations

There are a few safety considerations to take into account during both the manufacturing and testing of this product. As the final product includes a test fixture to encourage further research and testing, safety considerations regarding the manufacturing of new transducer chips and manifolds are apt to be mentioned. The process for manufacturing new transducer chips and manifolds requires the use of manual and CNC mills as well as SLA resin printers. Proper machining techniques and safety procedures must be followed throughout this process. These include, but are not limited to, the wearing of safety glasses, following machine shop rules and guidelines, and using best practices for each individual machine used. The assembly process for new chips involves the use of UV-cured resin and a UV flashlight. This should be done in a well-ventilated room, with care taken to wear protective gear so as not to expose oneself to

toxic uncured resin or potentially dangerous UV rays.

Once assembled, there are some additional safety factors to take into consideration during the testing process of new transducer chips, primarily with regards to the electrical components and setup. During a voltage testing configuration, there is no current running through the system. As such, the chances of harm related to this setup are very low. Despite this, care should still be taken to watch all electrical connections, especially between the electrodes and the voltmeter, to ensure they remain properly attached and there is no water seepage interfering with the connection points. When applying a load and testing for current, safety precautions should always be taken. It is recommended to reference a setup diagram to ensure proper electrical connections. As before, keeping a close eye on the test bed and electrodes to verify no water is leaking or interacting with the electrical components is necessary. While this product works in relatively low voltages and currents, it is still best practice to consider all possible instances of danger in the manufacturing or testing process and take all safety precautions possible to prevent or mitigate harm.

5.3   Engineering Standards

Standards are integral to engineering design as they provide universality and consistency across components and users, as well as the minimum expectations for safety and performance [Ref]. The following standards have been identified and considered as part of this project.

5.3.1   ASTM D6713-24 Standard Specification for Extruded and Compression Molded Shapes Made from Polyvinylidene Fluoride (PVDF)

This specification covers every aspect related to the requirements and test methods for the material properties, dimensions, and quality of workmanship for PVDF. This standard provided information and confidence in the properties and dimensioning of the PVDF used in this project. This was crucial for the machining and testing of the transducer chip, as well as for the initial selection of PVDF.

5.3.2   IEC 60038 IEC Standard Voltages, Consolidated Version

This IEC standard presents the standard voltage outputs for many different pieces of equipment. The standard provided a baseline voltage comparison for the testing and verification of the results for the final product presented here.

5.3.3   IEC 61010 Safety Requirements for Electrical Equipment for Measurement, Control, and Laboratory Use

The IEC Safety Requirements for Laboratory Use outline the standardized voltage testing procedures as well as the safety precautions required for laboratory testing and equipment. As this project hinges on the testing and verification of voltage outputs, this is a valuable and applicable standard for ensuring that all tests and testing equipment are consistent with regulation.

5.3.4 EPA Clean Water Act and Marine Debris Research, Prevention and Reduction Act

The Clean Water and Marine Debris Research, Prevention and Reduction Acts outline the basic requirements for any possible pollutant entering US waters. As this final product has the possibility of being used in a natural water setting in the United States to generate voltage from the inherent flow of currents or rivers, the materials used must adhere to the guidelines set forth by the EPA.

5.4 Societal Impact

Ocean and water based energy devices have long been used by humans as vast resources for clean, renewable energy. Most of these devices rely on the movement of waves and tides to move mechanical elements such as turbines. The only other significant contributor to water-based energy generation is in the form of dams [Ref]. Dams use a similar principle, however, and rely on tides or water reservoirs to turn turbines and generate electricity. This product and the scientific principles behind it are a new addition to the standard ways of generating electricity from ocean energy. This work has taken the exploration of ocean-based energy research into a new direction by relying on the inherent chemical properties of salt water and the movements of natural water sources, rather than simply mass movement.

Aside from the scientific principle driving it, the final design has a number of characteristics that make it unique in the field of voltage generation. Most notably, the final transducer chip design has no moving parts to it, aside from the flow of water through. With fewer moving parts than a mechanical component such as a turbine, this product requires less maintenance and can more passively generate voltage. Additionally, the chip's compact ratio of size to voltage generation allows for a uniquely large output to relatively small footprint. When placed into a natural moving water source, particularly one with a high flow rate, the chip becomes a compact, eco-friendly, low maintenance, clean energy source.

The potential societal impacts of new research into clean energy are significant. Renewable, affordable, and clean energy is one of the larger engineering crises and one of the seventeen United Nations' Sustainable Development Goals. As fossil fuels continue to run out and actively harm the planet, a switch to renewable and sustainable energy will become critical. This device could push another small step forward in affordable, renewable energy research and development. A secondary impact of this final product is in deep ocean research. With an array of transducer chips using the natural water flow of the ocean, deep sea exploration devices could naturally recharge their batteries to go deeper and further than before, without the need for resurfacing. Further ocean exploration and research would benefit scientific and engineering communities alike, leading to further understanding and development in these fields.

5.5 Lessons Learned

Many lessons were learned throughout the engineering process of this project, in regards to both the design process and team management. Perhaps the most important of these was a lesson in the power of iterative design. Iterative designing and rigorous testing is at the heart of any well-engineered product. Every improvement made to the final product was discovered

through a continuous process of designing, manufacturing, testing, analyzing, and redesigning. Through the course of this project, the design went through several iterations, each one building upon the last. Through challenges such as continued water leakage, low flow rates, or low voltage outputs, iterative design was the key to overcoming and moving on with the project. Whether it was improving the sealing geometry of the chip or finding new materials to produce a higher voltage, each iteration taught a lesson in and of itself, without which the final product would have been incomplete.

The opportunity to patent this final design also became an excellent learning experience on the design process and invention of a new product. There are a number of specific requirements and nuances as to which ideas could be candidates for a patent, who owns those ideas, and how to properly complete a patent application. Speaking with attorneys and working with Prof. Bandaru and Prof. Gillett through the patent process was an invaluable experience that revealed some of the inner workings of the engineering design and invention process.

Aside from the lessons learned within the engineering process itself, a great deal was learned regarding team management and effective, professional communication. The most productive work occurred when each team member played to their individual strengths and did their personal best. Combined with proper communication on what has been accomplished and what has yet to be completed, this strategy led to success in both completing the project in a timely manner and enjoying working together as a team. The lessons learned here will carry on through any and all future engineering endeavors made by the team.

References

[1] U.S. Geological Survey. (n.d.). *How much water is there on Earth?* [Website]. U.S. Department of the Interior. https://www.usgs.gov/special-topics/water-science-school/science/how-much-water-there-earth

[2] S.A. Sannasiraj, V. Sundar, *Assessment of wave energy potential and its harvesting approach along the Indian coast*, Renewable Energy, Volume 99, 2016, Pages 398-409, ISSN 0960-1481, https://doi.org/10.1016/j.renene.2016.07.017.

[3] Snowberg, D., Philip, R. T., Weber, J. (2024). Marine energy technology development risk management framework (Technical Report No. NREL/TP-5000-90212). National Renewable Energy Laboratory. https://www.nrel.gov/docs/fy24osti/90212.pdf.

[4] Qing Chang, *Chapter 7 - Electrical Properties*, Editor(s): Qing Chang, Colloid and Interface Chemistry for Water Quality Control, Academic Press, 2016, Pages 79-136, ISBN 9780128093153, https://doi.org/10.1016/B978-0-12-809315-3.00007-4.

[5] Fan, B., Bhattacharya, A., Bandaru, P. R. (2018). *Enhanced voltage generation through electrolyte flow on liquid-filled surfaces.* Nature Communications, 9(1), 4050. https://doi.org/10.1038/s41467-018-06297-9

[6] Xu, Y., et al. (2021). *Electrokinetic potential of liquid-filled surfaces for energy harvesting.* Langmuir, 37(14), 4342-4350. https://doi.org/10.1021/acs.langmuir.1c00738

[7] Zhang, Y., et al. (2020). *Advances in electrokinetic energy harvesting and its applications.* Journal of Materials Chemistry A, 8(25), 13114-13134. https://doi.org/10.1039/D0TA02410B

Acknowledgments

Appendix

5.6 Project Management

5.6.1 Task Distribution

1. Mamie Grace Barnard: Manufacturing and Assembly
2. Ashley Campbell: Testing and Data Acquisition
3. Markus Gokan: Design, CAD, and Assembly
4. Justin Kwak: Testing and Data Acquisition
5. Gabrielle Scott: Design, CAD, and Assembly
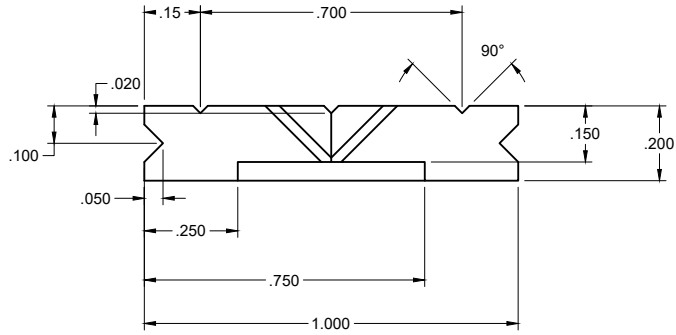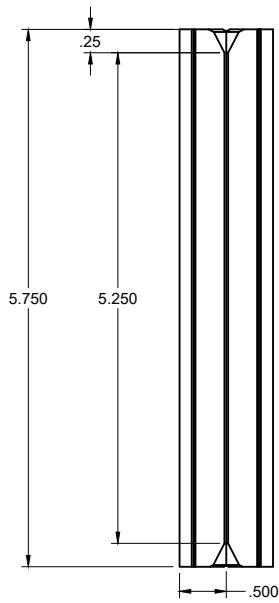
5.6.2 Individual Component Analyses

1. Mamie Grace Barnard: Electrodes
2. Ashley Campbell: Biofouling
3. Markus Gokan: Materials
4. Justin Kwak: Unit Cell Design
5. Gabrielle Scott: Manufacturing Methods

5.6.3 Intermediate Deadlines

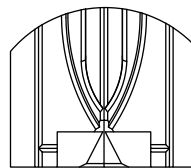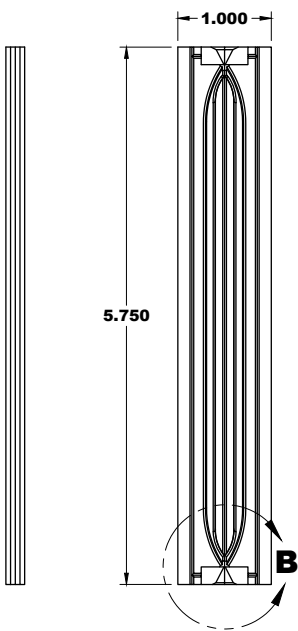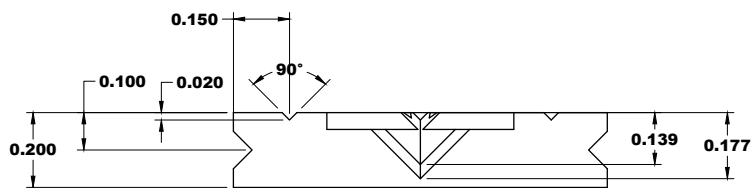| Task	Date
Initial ideas and first prototype	November 18, 2024 – November 22, 2024
Redesigning and material research	January 6, 2025 – January 10, 2025
Ordered PVDF, initial manufacturing of first iteration final design	January 22, 2025
First iteration final design testing (0.8 V result)	January 23, 2025
Redesigning and manufacturing second iteration final design	January 24, 2025 – January 30, 2025
First iteration testing and results reported to the DOE	Date of DOE submission
Second iteration final design testing	January 31, 2025
Final redesign and initial manufacturing, five channel chip manufacturing	February 17, 2025 – February 19, 2025
Presentation and verification of results with DOE	February 20, 2025
Identify and order new pump, assembled test fixture	February 23, 2025 – February 28, 2025
Final iteration manufacturing and data collection	March 3, 2025 – March 15, 2025

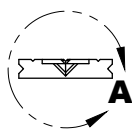Table 5.1: Project Timeline

5.7 Engineering Drawings

.25

5.750

5.250

.500

.15 .700 90°

.020

.100

.050

.250

.750

1.000

.150

.200

DETAIL A
SCALE 4:1

A
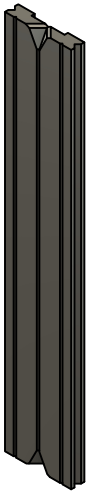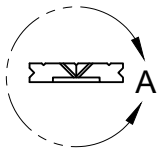
PROJECT				
MAE 156A				
TITLE				
v4 Chip				

APPROVED	SIZE	CODE	DWG NO	REV
CHECKED	B			
DRAWN Gabrielle Scott 3/11/2025	SCALE 1:2	WEIGHT	SHEET 1/1	

1.000

5.750

DETAIL B
SCALE 2:1

0.150

0.100 — **0.020**

90°

0.200

0.139 **0.177**

DETAIL A
SCALE 4:1

B

A

PROJECT			
MAE 156A			
TITLE			
v4 Chip 5 channel			

APPROVED	SIZE	CODE	DWG NO	REV
CHECKED	B			
DRAWN Gabrielle Scott 3/11/2025	SCALE 1:1	WEIGHT	SHEET 1/1	

SECTION B-B
SCALE 1:1

0.075

4X R0.300

1.700

B B

0.290

1.040

0.750

1.940

0.345

4X Ø0.177

4X Ø0.600

Ø0.375

Ø0.200

0.200

1.300

0.250

1.190

0.195

0.495

DETAIL A
SCALE 2:1

R0.100

0.750

0.650

0.200

0.045

A

A

45°

0.037

0.094

0.030

0.053
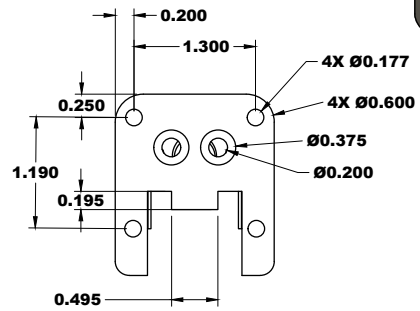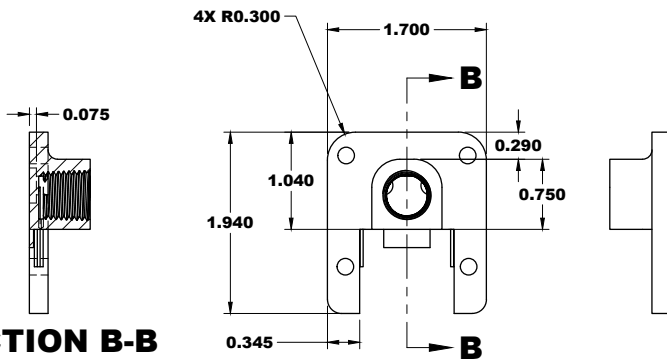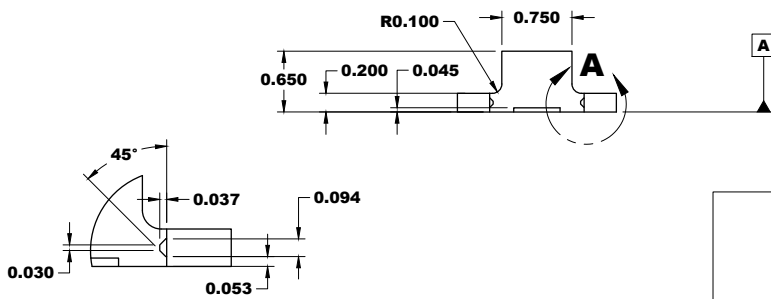
PROJECT				
MAE 156A				
TITLE				
v4 Cap				
APPROVED		SIZE	CODE	DWG NO	REV
CHECKED		B			
DRAWN	Gabrielle Scott	3/12/2025	SCALE 1:1	WEIGHT	SHEET 1/1

DETAIL B
SCALE 2:1

45°
0.037
0.094
0.030
0.053

1.700
2X Ø0.305
2X Ø0.205
1.940
1.040
1.235
0.400
0.345
0.495

0.200
1.300
4X R0.300
0.250
1.190
0.200
4X Ø0.177

A
B

DETAIL A
SCALE 2:1

0.222
45°
0.080
0.070
0.020
0.073
Ø0.039
0.100
0.090
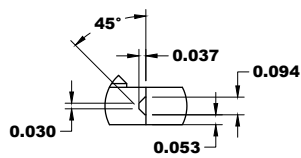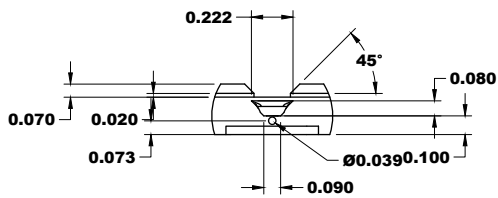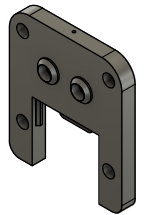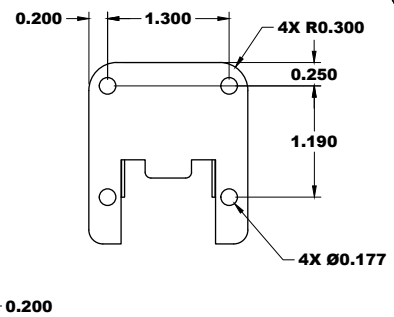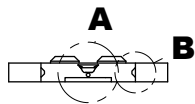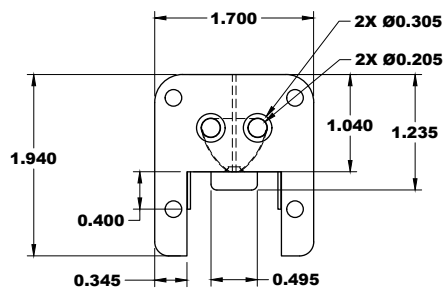
PROJECT	
MAE 156A	
TITLE	
V4 Base	

APPROVED	SIZE	CODE	DWG NO	REV
CHECKED	B			
DRAWN Gabrielle Scott 3/12/2025	SCALE 1:1	WEIGHT	SHEET 1/1	

PARTS LIST			
ITEM	QTY	PART NUMBER	MATERIAL
1	2	V4 MANIFOLD	STEEL
2	3	V4 CHIP BAD	STEEL
3	2	V4 BASE	STEEL
4	2	V4 CAP	STEEL
5	1	V4 BOTTOM PLATE	STEEL
6	1	V4 TOP PLATE	STEEL
7	1	TESTFIXTUREASSEM	STEEL
8	6	7397N19_UNIVERSAL-THREAD PUSH-TO-CONNECT TUBE FITTINGS	STEEL
9	1	COMPONENT3	
10	1	COMPONENT4	STEEL
11	1	COMPONENT6	STEEL

PROJECT
MAE 156A

TITLE
V3 Assembly

APPROVED		SIZE	CODE	DWG NO		REV
CHECKED		B				
DRAWN	Gabrielle Scott 3/11/2025	SCALE 1:2	WEIGHT		SHEET 1/1	

PARTS LIST			
ITEM	QTY	PART NUMBER	MATERIAL
1	2	V4 MANIFOLD	STEEL
2	3	V4 CHIP BAD	STEEL
3	2	V4 BASE	STEEL
4	2	V4 CAP	STEEL
5	1	V4 BOTTOM PLATE	STEEL
6	1	V4 TOP PLATE	STEEL
7	1	TESTFIXTUREASSEM	STEEL
8	2	7397N19_UNIVERSAL-THREAD PUSH-TO-CONNECT TUBE FITTINGS	STEEL

PROJECT
MAE 156A

TITLE
manifold_assembly_exploded

APPROVED		SIZE	CODE	DWG NO		REV
CHECKED		B				
DRAWN	Gabrielle Scott 3/12/2025	SCALE 1:2		WEIGHT	SHEET 1/1	

5.8 Part Listings

Section	Item	Quantity
Transducer Chip	PVDF sheet 6" x 6" x 1/4"	1
Manifold	SLA printed base manifold	2
Manifold	SLA printed cap manifold	2
Manifold	Soft Viton Fluoroelastomer O-Ring, 1/16 Fractional Width	4
Test Bed	Stainless Steel sheet 7" x 3" x 1/8" for clamping plate	2
Test Bed	M4 press fit nuts for clamping plate	12
Test Bed	M4 bolts for clamping plate	16
Test Bed	Silicone Rubber Strip, 10A Durometer, 1" x 36" x 0.010"	1
Test Bed	UV Resin	1
Test Bed	Permatex Form-a-Gasket Sealant	1
Test Bed	Silver Wire 24 Gauge 5 feet	1
Test Fixture	Universal Thread Push-to-Connect Tube Fitting	4
Test Fixture	Silicone Tubing 1/8 Inch ID x 1/4 Inch OD x 16.4 Feet	1
Test Fixture	Acrylic plate for base 8" x 8" 1/2"	1
Test Fixture	Acrylic plate flow meter mount 8" x 8" 1/4"	1
Test Fixture	SLS printed bracket for acrylic flow meter mount	2
Test Fixture	M4 heat-set threaded insert	12
Test Fixture	M4 bolts for acrylic plate	8
Test Fixture	Panel-Mount Flowmeter 4-44 GPH	1
Test Fixture	Panel-Mount Flowmeter 0.7-7 GPH	1
Test Fixture	Water Pump, Flow Rate 2L, Power 30W, Pressure Value 60 PSI	1
Test Fixture	Water Jug 5 Gallon	2

Table 5.2: Bill of Materials

5.9 List of Suppliers and Purchased Parts

Item	Supplier
High-Strength PVDF Sheet x2	McMaster-Carr
High-Temperature Ultra-Thin Silicone Rubber Strip, 10A Durometer, 1" x 36", 0.010" Thick	McMaster-Carr
Soft Viton Fluoroelastomer O-Ring, Chemical-Resistant, 1/16 Fractional Width, Dash Number 010, Packs of 25	McMaster-Carr
Panel-Mount Flowmeter with Flow-Control Knob, 4-44 GPH	McMaster-Carr
Panel-Mount Flowmeter with Flow-Control Knob, 0.7-7 GPH	McMaster-Carr
24 Gauge .999 Fine Silver Round Wire 0.020" 5 feet	Amazon
Silicone Tubing 1/8 Inch ID X 1/4 Inch OD X 16.4 Feet High Temp Hose Tube	Amazon
Electric Water Pump for 5 Gallon Flow Rate 2L Power 30W Pressure Value 60 PSI	Amazon

Table 5.3: List of Components and Suppliers
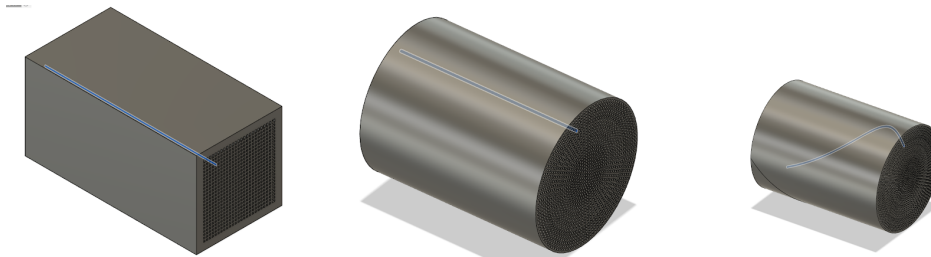
5.10 Designs Considered

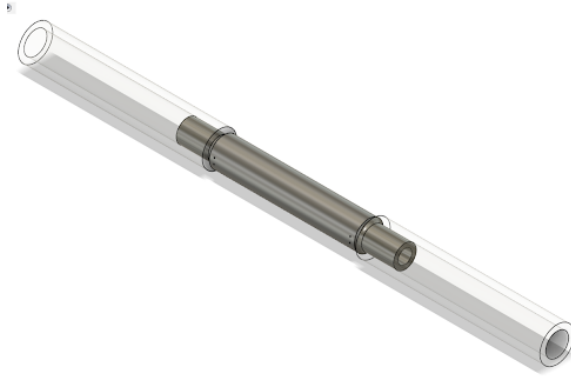Figure 5.1: Preliminary microchannel geometry design ideas.

Figure 5.2: Preliminary transducer chip design with original channel geometry connecting to flexible tubing.
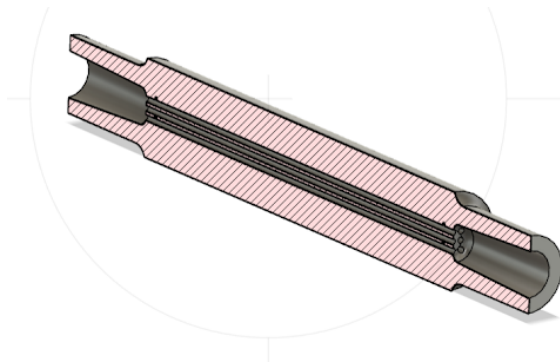

Figure 5.3: Cross-sectional view of preliminary transducer chip design.

Figure 5.4: Preliminary transducer design prototype with copper electrodes.
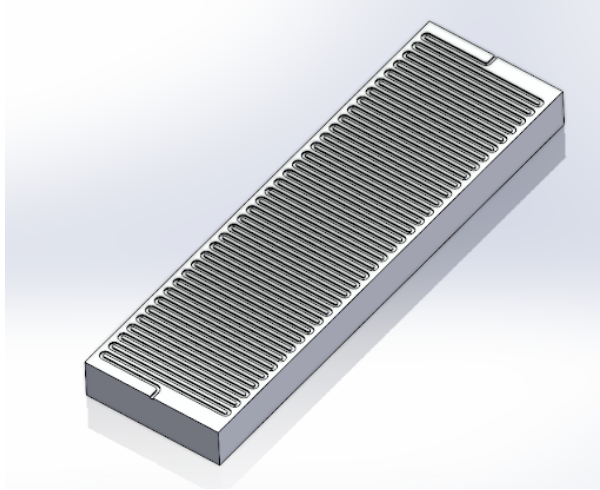
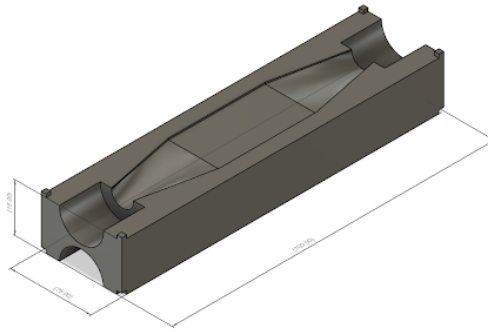Figure 5.5: Second iteration of microchannel geometry design.

Figure 5.6: First test bed iteration to contain newly designed transducer chip.
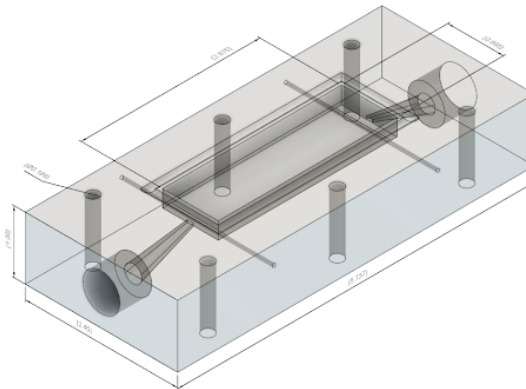

Figure 5.7: Base component of second test bed iteration to contain newly designed transducer chip.
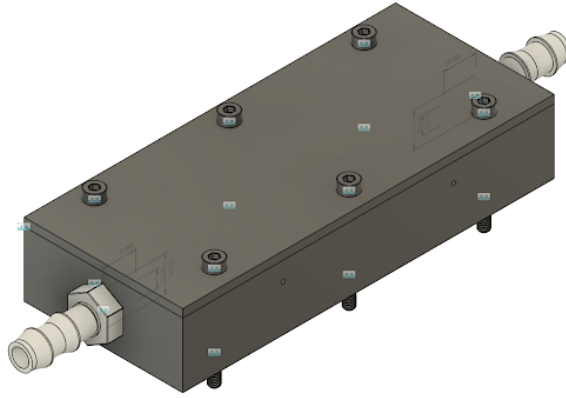
Figure 5.8: Full assembly of second test bed iteration with clamping components to contain newly designed transducer chip.
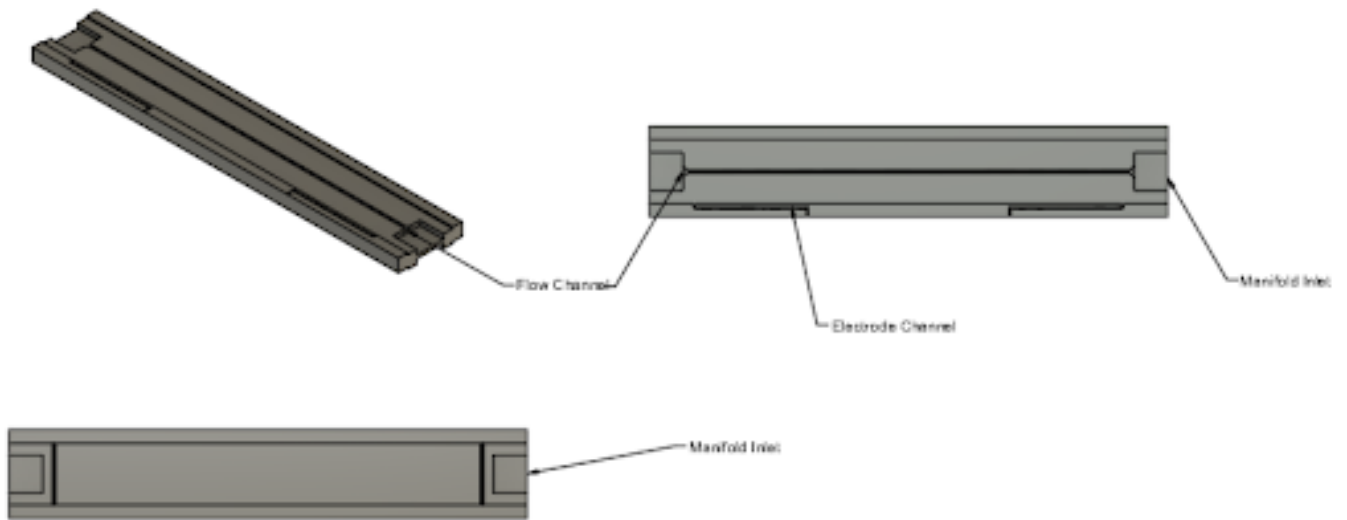

Figure 5.9: Third iteration of transducer chip. Features inlet recess to channel flow.
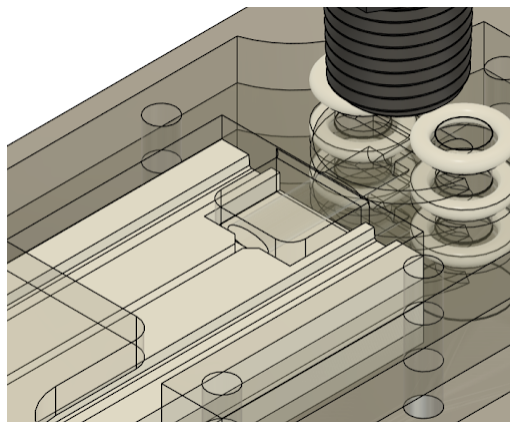

Figure 5.10: Inlet into third iteration transducer chip from newly designed mating manifolds.

Figure 5.11: Machined third iteration PVDF chips.
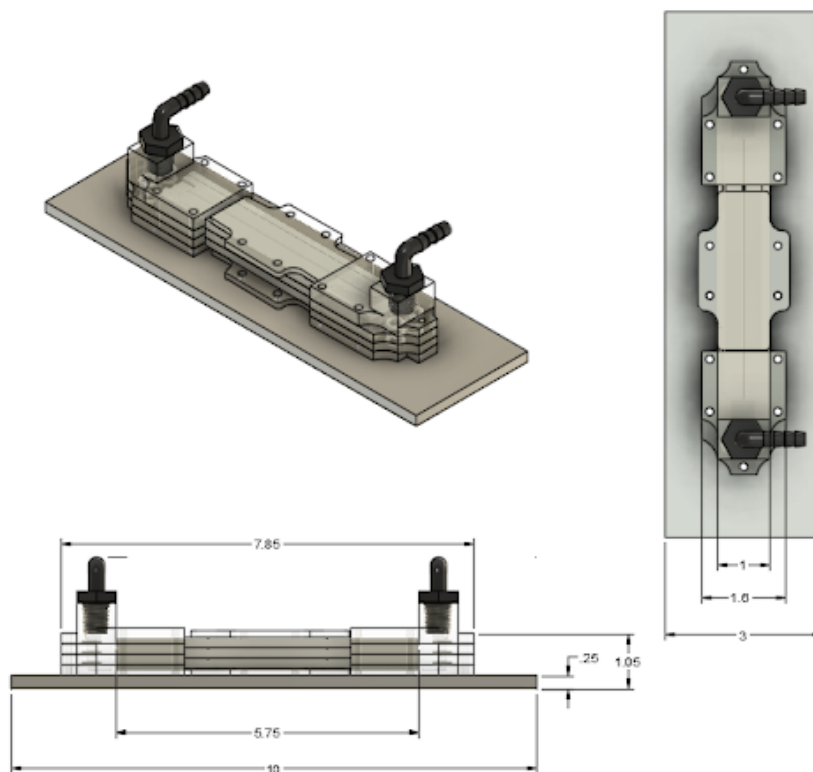
Figure 5.12: CAD model of test bed, featuring manifolds, rectangular transducer chips, clamping plates, and hose barbs.
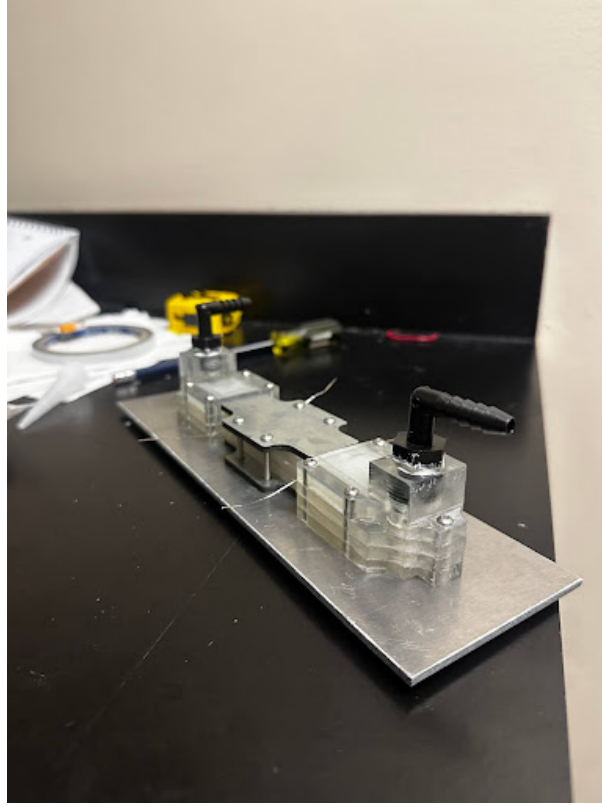
Figure 5.13: First fully manufactured and assembled test bed.

5.11   Equations and Formulas

$$V_s = \frac{\varepsilon \cdot \zeta}{\mu \cdot K} \cdot \Delta P \qquad (5.1)$$

$$I_s = \frac{K \cdot \pi \cdot r^2}{L} \cdot V_s \qquad (5.2)$$

$$\Delta P = \frac{32 \cdot \mu \cdot L \cdot Q}{\gamma \cdot D_h^4} \qquad (5.3)$$

$$K = \frac{32 \cdot A^2}{\gamma \cdot D_h^4} \qquad (5.4)$$

$$V_s = \frac{\varepsilon \cdot \zeta \cdot L \cdot Q}{A^2} \qquad (5.5)$$

$$I_s = \frac{8 \cdot \pi \cdot \varepsilon \cdot \zeta \cdot Q}{\gamma \cdot D_h^2} \qquad (5.6)$$

$$V_s = \frac{\varepsilon \cdot \zeta \cdot L \cdot Q}{A^2} \tag{5.7}$$

$$\zeta = \frac{V_s \cdot A^2}{\varepsilon \cdot L \cdot Q} \tag{5.8}$$

$$\zeta = \frac{V_s \cdot A^2}{\varepsilon \cdot L \cdot Q} \tag{5.9}$$

$$V_s = \frac{\varepsilon \cdot \zeta \cdot L \cdot Q}{A^2} \tag{5.10}$$

$$I_s = \frac{8\pi\varepsilon\zeta Q}{\gamma D_h^2} \tag{5.11}$$

5.12 Calculations

Flow Meter Range: 0.7-7GPH										
Channels:	1 m/s	2 m/s	3 m/s	4 m/s	5 m/s	6 m/s	7 m/s	8 m/s	9 m/s	10 m/s	Graduation
1	0.24	0.48	0.71	0.95	1.19	1.43	1.66	1.90	2.14	2.38	0.24
3	0.71	1.43	2.14	2.85	3.57	4.28	4.99	5.71	6.42	7.13	0.71
5	1.19	2.38	3.57	4.76	5.94	7.13	8.32	9.51	10.70	11.89	1.19
10	2.38	4.76	7.13	9.51	11.89	14.27	16.64	19.02	21.40	23.78	2.38
15	3.57	7.13	10.70	14.27	17.83	21.40	24.96	28.53	32.10	35.66	3.57
Flow Meter Range: 4-44GPH										
Channels:	1 m/s	2 m/s	3 m/s	4 m/s	5 m/s	6 m/s	7 m/s	8 m/s	9 m/s	10 m/s	Graduation
1	0.24	0.48	0.71	0.95	1.19	1.43	1.66	1.90	2.14	2.38	0.24
3	0.71	1.43	2.14	2.85	3.57	4.28	4.99	5.71	6.42	7.13	0.71
5	1.19	2.38	3.57	4.76	5.94	7.13	8.32	9.51	10.70	11.89	1.19
10	2.38	4.76	7.13	9.51	11.89	14.27	16.64	19.02	21.40	23.78	2.38
15	3.57	7.13	10.70	14.27	17.83	21.40	24.96	28.53	32.10	35.66	3.57

5.13 Budget

Item	Cost	Date Purchased
High-Strength PVDF Sheet, 6" x 6" x 1/4" x1	$76.09	1/13/2025
Water- and Steam-Resistant High-Temperature EPDM O-Ring, 1/32 Fractional Width, Dash Number 001-1/2, Packs of 100 x1	$9.38	1/17/2025
Soft Viton Fluoroelastomer O-Ring, Chemical-Resistant, 1/16 Fractional Width, Dash Number 010, Packs of 25	$7.09	1/17/2025
High-Temperature Soft Silicone O-Ring Cord Stock 1/16 Fractional Width, 0.07" Actual Width, 3 ft. Length x2	$5.28	1/17/2025
High-Strength PVDF Sheet, 6" x 6" x 1/4" x2	$125.08	1/24/2025
Plastic Barbed Hose Fitting for Water, Elbow, 1/4" Hose ID, 1/4 NPT Male, 150 PSI x6	$9.60	1/24/2025
Plastic Barbed Hose Fitting for Water, Tee Connector for 1/4" Hose ID x4	$7.40	1/24/2025
Plastic Barbed Hose Fitting for Water, Tee Adapter for 1/4" Hose ID, 1/4 NPT Male x6	$9.06	1/24/2025
High-Temperature Ultra-Thin Silicone Rubber Strip x1	$19.57	2/12/2025
High-Purity High-Temperature Silicone Rubber Strip, 1" x 36", 0.005" Thick x1	$6.30	2/12/2025
Printed Veroclear Manifolds	$27.99	2/18/2025
24 Gauge .999 Fine Silver Round Wire 0.020" 5 feet	$22.76	2/24/2025
Silicone Tubing 1/8 Inch ID X 1/4 Inch OD X 16.4 Feet High Temp Hose Tube	$12.69	2/24/2025
Electric Water Pump for 5 Gallon Flow Rate 2L Power 30W Pressure Value 60 PSI	$57.69	2/24/2025

Table 5.4: Project Purchases and Costs